

# Nanomaterials for Diagnosis: Challenges and Applications in Smart Devices Based on Molecular Recognition

Oswaldo N. Oliveira, Jr.,<sup>\*,†</sup> Rodrigo M. Iost,<sup>‡</sup> José R. Siqueira, Jr.,<sup>§</sup> Frank N. Crespilho,<sup>‡</sup> and Luciano Caseli<sup>||</sup>

<sup>†</sup>São Carlos Institute of Physics, University of São Paulo, CP 369, 13560-970 São Carlos, São Paulo, Brazil

<sup>‡</sup>São Carlos Institute of Chemistry, University of São Paulo, CP 380, 13560-970 São Carlos, São Paulo, Brazil

<sup>§</sup>Institute of Exact Sciences, Natural, and Education, Federal University of Triângulo Mineiro, 38025-180 Uberaba, Minas Gerais, Brazil

<sup>||</sup>Institute of Environmental, Chemical and Pharmaceutical Sciences, Federal University of São Paulo, 09972-270 Diadema, São Paulo, Brazil

**ABSTRACT:** Clinical diagnosis has always been dependent on the efficient immobilization of biomolecules in solid matrices with preserved activity, but significant developments have taken place in recent years with the increasing control of molecular architecture in organized films. Of particular importance is the synergy achieved with distinct materials such as nanoparticles, antibodies, enzymes, and other nanostructures, forming structures organized on the nanoscale. In this review, emphasis will be placed on nanomaterials for biosensing based on molecular recognition, where the recognition element may be an enzyme, DNA, RNA, catalytic antibody, aptamer, and labeled biomolecule. All of these elements may be assembled in nanostructured films, whose layer-by-layer nature is essential for combining different properties in the same device. Sensing can be done with a number of optical, electrical, and electrochemical methods, which may also rely on nanostructures for enhanced performance, as is the case of reporting nanoparticles in bioelectronics devices. The successful design of such devices requires investigation of interface properties of functionalized surfaces, for which a variety of experimental and theoretical methods have been used. Because diagnosis involves the acquisition of large amounts of data, statistical and computational methods are now in widespread use, and one may envisage an integrated expert system where information from different sources may be mined to generate the diagnostics.

**KEYWORDS:** *nanomaterials, biosensors, smart devices, molecular recognition, clinical diagnosis*



**NANOSCALE FOR BIOMEDICAL PURPOSES**

## 1. INTRODUCTION

A variety of tailored materials are now controlled on the nanoscale for biomedical purposes, including clinical diagnosis.<sup>1</sup> The composition and structure of these materials can be predefined to offer enhanced sensitivity for a given target by exploiting molecular-recognition interactions,<sup>2</sup> with the aim of making their electrical, magnetic, or optical property very sensitive to the analyte of interest. The assembly of different materials in a device is an important requirement for sensing, which depends on strategies to attach biomolecules or synthetic materials by physical adsorption or covalent binding. One such strategy consists of adsorbing nanomaterials and biomolecules in ultrathin films that functionalize solid substrates or colloidal particles. This is the reason why methods to investigate interfaces<sup>3</sup> and to produce nanostructured films with control on the molecular level<sup>4</sup> have become increasingly important for biosensing. Another possibility is the use of nanomaterials in solutions or dispersions, as in the case of metallic or magnetic

nanoparticles conjugated with biomolecules that are selective to cancer cells.<sup>5</sup>

Regardless of the way the biomolecules are assembled in devices for biosensing and clinical diagnosis, the key concept is molecular recognition, which is also essential for many biological processes. Important examples are the specific interaction between an enzyme and its substrate to catalyze reactions, the recognition of complementary bases in nucleic acids through hydrogen bonding to form DNA and RNA, and the interaction between amino acids and triads of nitrogen bases for forming proteins. Many of these processes involve supramolecular systems for which molecular recognition in living beings occurs mostly at interfaces, such as membrane surfaces, enzyme reaction sites, or in the inner part of the DNA double helix. Therefore,

**Received:** March 12, 2014

**Accepted:** June 26, 2014

**Published:** June 26, 2014

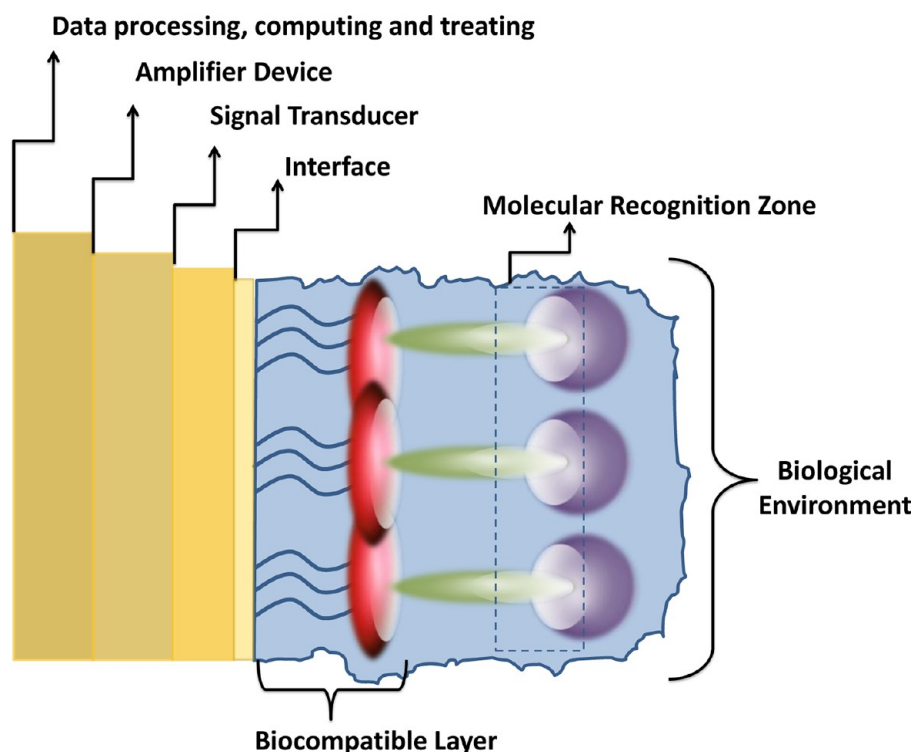


**Figure 1.** Schematic architecture for a biosensor based on molecular recognition.

relevant biological recognition processes occur at some kind of interface.

This review discusses the recent advances in the development of biosensors produced with materials organized on the nanoscale, with emphasis on new molecular architectures for smart devices applied to diagnostics and monitoring health treatments; it is organized as follows: Section 2 describes a generic architecture for biosensing in which nanomaterials are exploited, and the principles of detection are presented in Section 3. A long list of nanomaterials for biosensing and diagnosis is discussed in Section 4, where examples from the literature are given to illustrate the capabilities of these nanomaterials. A special section is devoted to smart devices, particularly, implantable biosensors. The need to employ statistical and computational methods to treat the large amounts of data generated in clinical diagnosis is discussed in Section 6, and final remarks close the paper in Section 7. It should be stressed that the coverage of the topic is not comprehensive; considering that ca. 1400 papers are retrieved in a search in the Web of Science with the entry “clinical diagnosis” and “nano\*”, we found it best to emphasize contributions for distinct types of nanomaterials.

## 2. A GENERIC ARCHITECTURE FOR BIOSENSORS BASED ON NANOMATERIALS FOR CLINICAL DIAGNOSIS

The architecture of a generic smart biosensor is depicted in Figure 1, from which one may highlight three essential components: (i) immobilized biomolecules capable of molecular recognition, which may be adsorbed on a biocompatible layer, (ii) signal transducers, and (iii) elements for measuring and amplifying the signal in addition to treating the data. The list of possible biomolecules in the molecular recognition zone and of analytes in the biological environment is immense and could include, e.g., antibody–antigen, enzyme–substrate, nucleic acids, and complementary base pairing in DNA.<sup>6–9</sup> Another important

ingredient in the biosensor is the so-called biocompatible layer, for it may also be considered as the matrix for immobilizing the biomolecules in order to preserve their activity.<sup>10</sup> The three most used methods for assembling nanomaterials for this purpose are the Langmuir–Blodgett (LB),<sup>11,12</sup> the electrostatic layer-by-layer (LbL),<sup>13,14</sup> and the self-assembly monolayer (SAM) techniques,<sup>15</sup> all of which allow one to assemble materials in a layer-by-layer fashion.

The example of biosensor in Figure 1 appears to imply that the biomolecules should be immobilized on a solid support. However, other possibilities exist, which include biomolecules adsorbed on particles (even nanoparticles)<sup>16</sup> and nanostructures that function as reporters.<sup>17</sup> Also indicated in Figure 1 is the need for signal transduction, for which various methods can be used. These include optical techniques, normally with detection of a reaction product via absorption spectroscopy<sup>18</sup> or with vibrational spectroscopy,<sup>19</sup> in addition to imaging techniques,<sup>20,21</sup> mass detection,<sup>22</sup> surface plasmon resonance (SPR),<sup>23</sup> and electrical measurements.<sup>24</sup> With regard to biosensors based on electrical measurements, perhaps the most widespread are the electrochemical biosensors in which products from redox reactions are detected with, e.g., cyclic voltammetry<sup>25</sup> or amperometry.<sup>26</sup> Electrical impedance spectroscopy has found increased use in the past few years and has the potential to generate low-cost, fast diagnosis. As for the possible integration with microelectronics, detection may be performed by exploiting concepts used in field-effect devices.<sup>27</sup> In Section 3, we will discuss the advantages and limitations of these principles of detection.

One should also stress that the architecture of Figure 1 may be generalized to include an array of sensors for the detection task, rather than just one sensing unit as depicted. In fact, sensor arrays have been extensively explored over the past few years, especially in conjunction with impedance spectroscopy as principle of detection.<sup>28</sup> The various methods for signal amplification and

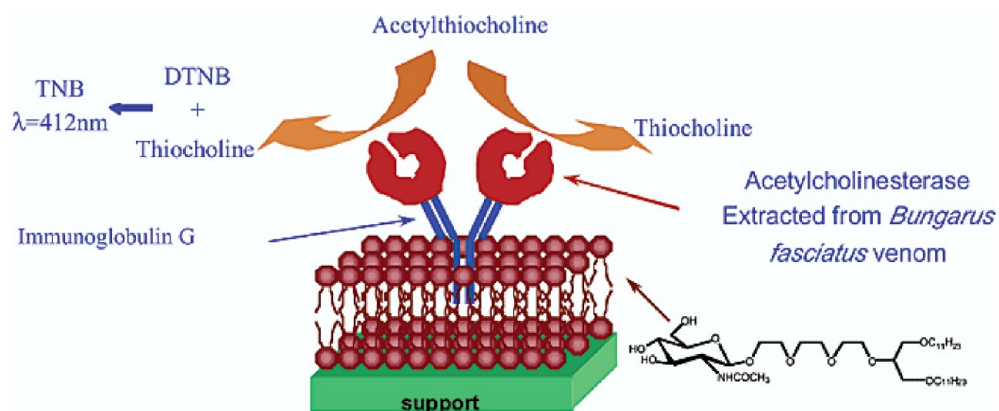


**Figure 2.** Schematic representation of the organized proteo-glycolipidic molecular assembly with oriented recognition sites. The acetylcholinesterase activity was monitored with colorimetry. Reprinted with permission from ref 40. Copyright 2003 American Chemical Society.

data processing, available for other tasks, may be used for biosensing. In Section 6, we will concentrate on new trends for data processing, in which artificial intelligence and information visualization methods are combined to enhance the performance of biosensors.

**2.1. Assembling Nanomaterials.** Because molecular recognition tends to take place at interfaces, biosensing relies mostly on adsorbed biomolecules in nanostructured films. As mentioned above, there are three methods that are the most popular for this purpose, namely, the LB and LbL techniques and the SAM monolayers. Their most important features, as far as biosensing is concerned, are the possible control of molecular architectures and the mild conditions under which the films are fabricated.<sup>29</sup> The latter is essential for preserving the activity of the biomolecules, which is probably associated with entrained water that remains in the films even after drying.

The LB method is based on the transfer of insoluble materials from monolayers at the air–water interface onto solid supports that intercept the monolayer vertically.<sup>30,31</sup> It was primarily conceived to produce well-ordered multilayers of lipids,<sup>32–34</sup> but over decades many other types of molecules have been employed. Its use for biosensing involves immobilization of proteins, especially enzymes,<sup>35</sup> in addition to antibodies<sup>36</sup> and DNA.<sup>37</sup> In many cases, the biomolecules are embedded in a lipid matrix whose role is to preserve bioactivity. Indeed, even though immobilization can restrict chain mobility and decrease enzyme activity, in other instances the hydrophobic environment provided by lipid–enzyme mixed LB films offers a way to better expose the catalytic site of the enzyme to the analytes, thus enhancing the catalytic activity.<sup>38,39</sup>

A typical biosensor based on an LB film is shown schematically in Figure 2, where a functionalized bilayer should provide a unique orientation for the recognition sites. In this example, the lipid bilayer comprises a neoglycolipid with highly fluid hydrocarbon chains, onto which the immunoglobulin (IgG) antibody is anchored. Carbohydrate interactions between the glycan moieties of IgG and the glycolipid headgroup are favored, in addition to the probable hydrophobic interactions between fragments of IgG and the lipid moiety of the glycolipid leaflets. Acetylcholinesterase was coupled to the bilayer by immune association, and this biosensor was employed to detect thiocoline via colorimetric methods.<sup>40</sup>

The LbL technique is complementary to the LB method, having been conceived for water-soluble materials in contrast to the insoluble monolayers transferred as LB films. In the LbL

technique, adsorption of multilayers is governed by noncovalent interactions, especially electrostatic attraction between oppositely charged species. In the seminal work introducing the LbL technique, polyelectrolytes were used,<sup>13</sup> but this has been extended to many other materials, which include inorganic nanoparticles in addition to organic materials (for a review, see ref 41). With experiments involving such a variety of materials, it was then found that LbL films could also be built with H-bonding interactions and other types of noncovalent interactions.<sup>42</sup> This versatility is indeed one of the major advantages of the LbL method, which may be used to coat any type of support of any shape, from solid plates to microparticles and nanoparticles.<sup>43</sup>

Numerous materials in LbL films are used for biosensing, including carbon nanotubes (CNTs),<sup>44</sup> graphene sheets,<sup>45</sup> metal nanoparticles,<sup>46</sup> and biomolecules.<sup>47</sup> Of particular importance in this regard is the control of molecular architecture, as exemplified in the biosensor schematically shown in Figure 3. The main aim in this specially designed architecture was to provide a friendly environment for adsorption of glucose oxidase (GOx) in order to detect glucose at a low potential and with high sensitivity. Also,

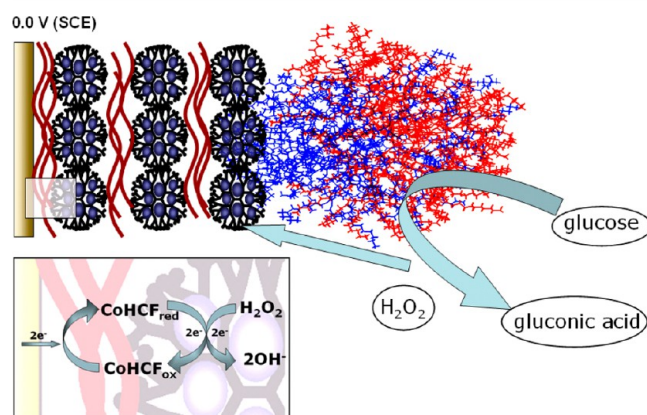


**Figure 3.** Biosensor especially designed to detect glucose via determination of  $\text{H}_2\text{O}_2$ , as indicated in the reaction depicted. Its architecture is composed of an LbL film deposited onto an ITO substrate, namely, ITO-(PVS/PAMAM-Au)<sub>3</sub>@CoHCF-GOx electrode. The gold nanoparticles were incorporated to lead to an increased current and therefore enhanced sensitivity, and they were coated with the CoHCF redox mediator in order to allow detection at 0.0 V vs SCE. The enzyme glucose oxidase (GOx) was immobilized in a friendly environment obtained with a solution containing BSA and glutaraldehyde. Modified with permission from ref 47. Copyright 2006 Elsevier.

glucose detection was via determination of  $\text{H}_2\text{O}_2$  resulting from the reaction with glucose catalyzed by GOx, from which gluconic acid was also generated. The catalytic reaction is indicated in the figure inset. In order to increase sensitivity, gold nanoparticles were incorporated into dendrimer layers. These nanoparticles were then coated with a redox mediator, thus allowing detection at 0.0 V vs SCE (saturated calomel electrode) and avoiding effects from interferents. As for providing a friendly environment, GOx was coimmobilized with bovine serum albumin. With regard to glucose sensing, this is a topic where nanomaterials show high sensing performance, and products are nearly ready for commercialization. A detailed evaluation of the sensing performance in comparison to non-nanomaterial based sensors is found in ref 48.

Self-assembled monolayers (SAMs) are formed by the spontaneous chemisorption of a variety of organic molecules on a surface, which may contain groups such as thiols, amines, acids, disulfides, and silanes.<sup>49</sup> The method has been developed over decades, following the seminal work by Sagiv in the 1980s.<sup>50</sup> One of the many SAM features exploited in biosensing is the ability to control the interface properties, with multiple tasks being performed by a single monolayer.<sup>51</sup> Other advantages include the high stability afforded by chemisorption and the higher control over positioning of biomolecules compared to that of polymer layers. Indeed, with SAMs, the position and density of the biomolecules can be controlled both vertically and laterally, which is not possible with LB or LbL films, for instance.

For biosensing, SAMs are normally functionalized by attaching ligands, which confers great flexibility for the choice of the biomolecules to immobilize. Hence, SAMs can be utilized in enzyme electrodes, in functionalizing the gate in field-effect devices, in a variety of immunosensors, and for detecting DNA.<sup>52</sup> Figure 4 depicts a schematic diagram of SAMs to perform this latter task.

### 3. PRINCIPLES OF DETECTION

The choice of the detection method and variants of the techniques employed are crucial for biosensing, where one

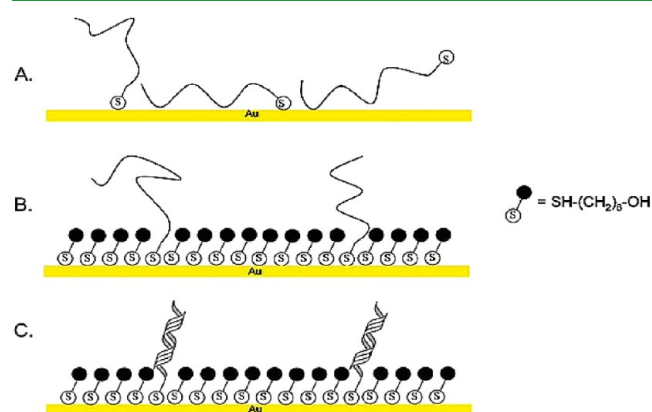


**Figure 4.** Molecular architecture for a DNA biosensor using self-assembled monolayers. (A) Single-stranded DNA (HS-ssDNA) is adsorbed on the gold substrate via the thiol end group and backbone/substrate contacts, thus leading to various adsorption states. (B) Contacts between the DNA backbone and the substrate are prevented by forming a mercaptohexanol (MCH) monolayer. HS-ssDNA remains attached by the thiol end. (C) Hybridization to complementary oligonucleotides takes place at the end-tethered HS-ssDNA. Reprinted with permission from ref 51. Copyright 2006 John Wiley & Sons, Inc.

must take into account the properties of the material in the sensing units and of the analyte. In this section, we highlight some of the most used methods for biosensing and clinical diagnosis.

**3.1. Electrochemical Detection and Electrodes for Diagnosis.** Electrochemical methods for biosensing are based on charge-transfer or charge-transport mechanisms, with changes in Faradaic or capacitive currents being used as a signal for detection, depending on the characteristics of the recognition element. Chronoamperometry and voltammetry are the most common among the Faradaic methods. Another useful parameter is a change in the electrochemical potential at the interfacial region. Owing to the variety of electrochemical methods used in biosensing, it is not practicable to cover them all here. Instead, we will concentrate on techniques that have been recently shown to be promising for clinical diagnosis. Emphasis will be placed on the preparation of electrodes and new insights into interfacial science.

In the procedures to detect biologically relevant analytes, one may gain localized electrochemical information with scanning electrochemical cell microscopy<sup>53,54</sup> (SECM), which even allows one to study the electrocatalytic properties of single nanoparticles. This has been reported by Kleijn and co-workers<sup>55</sup> with the approach shown schematically in Figure 5. A micropipette is filled with a solution of citrate-gold nanoparticles (AuNPs) (Figure 5a) with diameters ranging from 10 to 20 nm according to the TEM image in Figure 5c. The scanning probe moved in contact with the electrolyte, and AuNPs landed at various potentials using highly oriented pyrolytic graphite (HOPG), where redox reactions occurred, as indicated in Figure 5b. The carbon-coated TEM grid was also used to obtain information about nanoscale level measurements of single NPs. The voltammetric behavior at  $200 \text{ mV s}^{-1}$  for the corresponding single AuNPs with oxidation wave onset potential at 0.8 V in Figure 5d indicates high sensitivity with low background current. The SECM technique has been extended to biological molecules, such as enzymes and DNA.<sup>56</sup>

Mention should be made of miniaturized systems toward micro- and nanodevices exploring 0D, 1D, and 2D nanomaterials, including carbon nanotubes (CNTs), graphene sheets (GS),<sup>57–59</sup> and metallic nanoparticles.<sup>60</sup> Small-size ultramicroelectrodes (UME) have been also produced,<sup>61</sup> which have at least one of their dimensions in micrometers.<sup>62</sup> Further developments took place with nanometer-size materials with nanoelectrodes down to 100 nm fabricated with electron beam lithography, ion beam lithography, and photolithography.<sup>63,64</sup> With such electrodes, the ohmic drop ( $IR$ ) decreased, and they reached enhanced mass transport, fast kinetics in charge transfer, and high current density.<sup>65,66</sup> There are limitations, however, including a low current in the range from nano- to femtoamperes<sup>67</sup> and effects from the diffuse double layer in the mass transport of redox species. Besteman and co-workers<sup>68</sup> used single semiconducting CNTs for biosensing, with glucose oxidase (GOx) attached to their sidewalls. Still concerning nanodevices, biochips were built with an indium tin oxide nanowire (ITO-NW) modified with GOx enzyme,<sup>69</sup> as indicated in Figure 6.<sup>67</sup> Glucose could be detected with currents on the order of picoamperes being measured due to the biocatalytic process. With such small currents, special precautions had to be taken to identify and eliminate noise, which was done with numerical methods in dedicated software. Noise was essentially of thermal origin, in addition to shot noise. The treatment of the data permitted complete elimination of high-frequency signals.

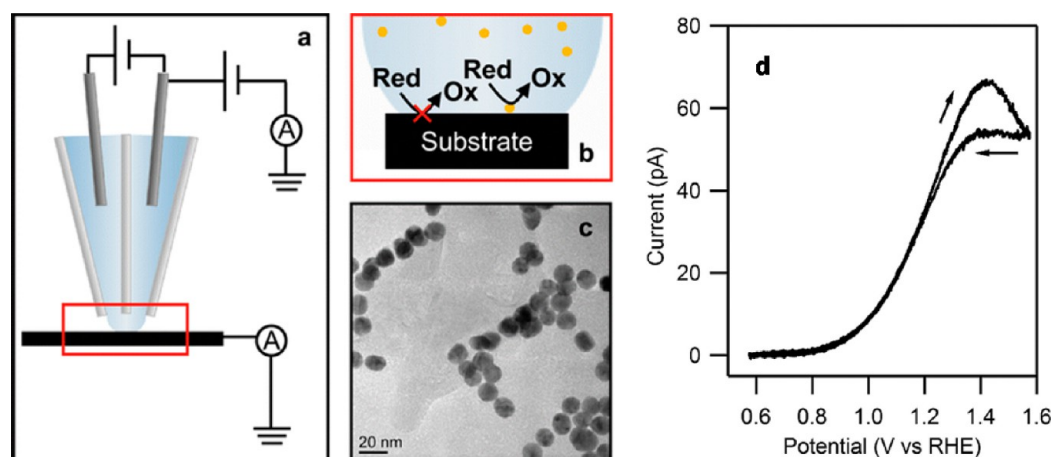


**Figure 5.** (a) Experimental setup, including the micropipette to dispense the nanoparticles. (b) Reaction on the substrate. (c) TEM image showing AuNPs. (d) Cyclic voltammogram taken at  $200 \text{ mV s}^{-1}$  for the individual AuNP. Reprinted with permission from ref 55. Copyright 2011 American Chemical Society.

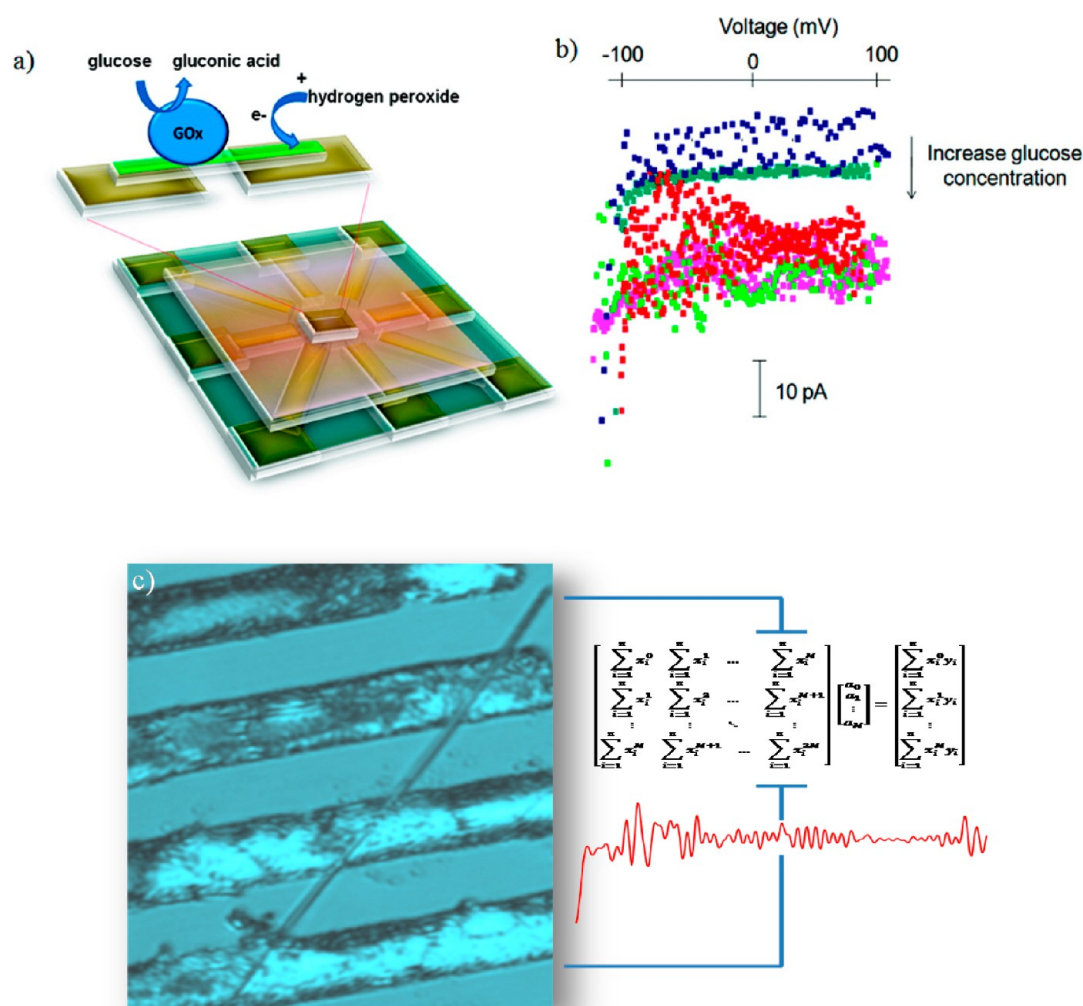


**Figure 6.** (a) Artistic representation of the device, with the inset showing the reaction responsible for detection. (b) Several plots of linear voltammetry are shown for the ITO-NW electrode with glucose concentrations (blue boxes,  $0.0 \mu\text{mol L}^{-1}$ ; dark green boxes,  $0.1 \mu\text{mol L}^{-1}$ ; orange boxes,  $0.2 \mu\text{mol L}^{-1}$ ; pink boxes,  $0.5 \mu\text{mol L}^{-1}$ ; and light green boxes,  $1.0 \mu\text{mol L}^{-1}$ ). (c) SEM image of the NW-ITO deposited on gold microswitches, whose width was  $4 \mu\text{m}$ . A typical signal is illustrated on the right side of the panel along with the mathematical formalism to analyze the signal. Reprinted with permission from ref 67. Copyright 2011 American Chemical Society.

**3.2. Impedance Spectroscopy.** Sensors based on impedance spectroscopy are advantageous because this principle of

detection offers a direct, label-free, and referenceless detection method. They function by applying an external ac electric field in

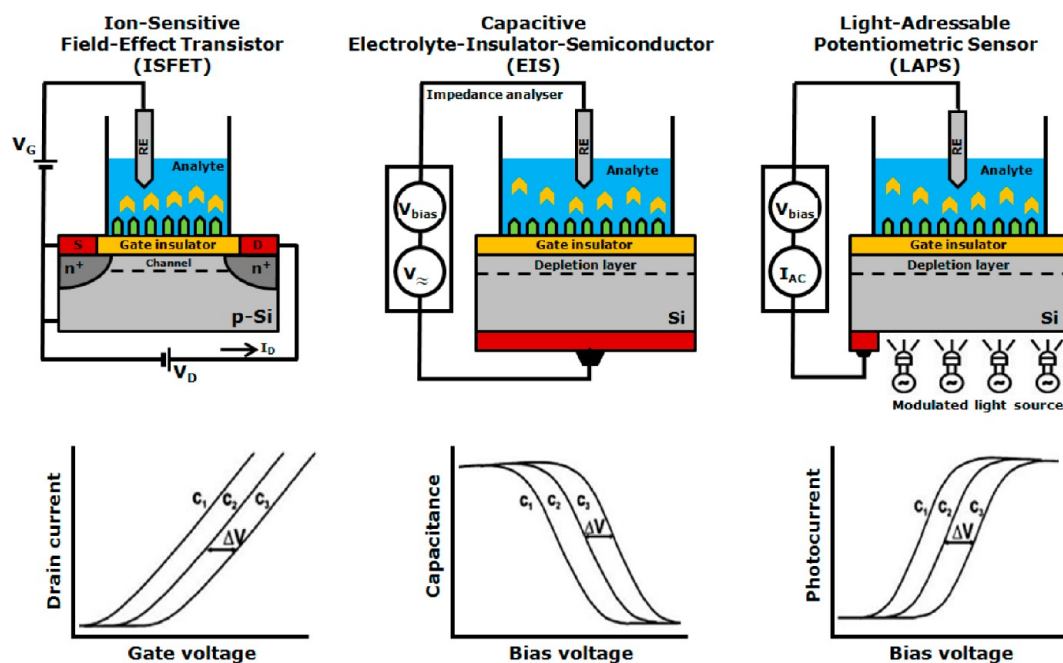


**Figure 7.** (Top) Operation principles for ISFET, EIS and LAPS sensors, from left to right, are shown schematically. (Bottom) Typical signal responses of the sensors shown in the top of the figure. Modified with permission from ref 71. Copyright 2006 John Wiley & Sons, Inc.

the sensing device, whose frequency can be varied to probe distinct mechanisms of charge storage and transport.<sup>70</sup> In practice, the film-forming dielectric material in the device is placed between capacitor plates, whose geometry may be varied at will. In the case of interdigitated electrodes, two pairs of metallic fingers are evaporated on a solid substrate, e.g., glass or ceramic plates, in a way that the dielectric material (e.g., nanomaterials and/or biomolecules) is deposited in the gaps of the metallic tracks. The electrical impedance of the electrodes coated with the film-forming material is highly sensitive to the interaction with analytes, and this can be used not only for liquid samples but also for vapors. Impedance spectroscopy can also be coupled with electrochemical measurements, which is exploited in field-effect devices, as mentioned below.

**3.3. Field-Effect Devices.** Because integration with microelectronics is a welcome feature for sensors and biosensors, there has been considerable research into the use of field-effect devices (FEDs). These devices are silicon-based sensors deriving from field-effect transistors (FETs), in which the gate electrode is replaced by an electrolyte solution and a reference electrode. The most obvious advantages of FEDs are associated with the possible integration of sensor arrays on a chip, thus allowing one to fabricate small, low-weight, and low-cost devices.<sup>70</sup> Typical examples of FEDs are the ISFETs (ion-sensitive field-effect transistors), capacitive EIS (electrolyte-insulator-semiconductor) sensors, and LAPS (light-addressable potentiometric sensors),<sup>71</sup> whose architectures are shown in Figure 7. These sensors are sensitive to any electrical interaction at or nearby the interface between the gate layer and the electrolyte. Upon inducing changes in the chemical composition of the analyte, one may modify the electrical surface charge of the FED, thus modulating the current of the ISFET channel, the capacitance of EIS, and the photocurrent of LAPS.<sup>71</sup> The signal in these sensors arises from changes in pH or ion concentration, which may result from an enzymatic reaction or from adsorption of charged species. Therefore, sensing is made possible with physical adsorption of macromolecules such as polyelectrolytes, proteins

and DNA, or with the binding of molecules in molecular recognition mechanisms, including antigen–antibody affinity reactions and DNA hybridizations.<sup>70,71</sup>

The integration of nanomaterials and biological systems into FEDs is suitable for detection of biological species, mainly due to the size compatibility and the possibility of integration in microchips. In addition, the electrostatic interactions and charge transfer, typical of biological processes, may be detected by electronic nanocircuits.<sup>72</sup> This integration has normally been done with the LbL technique, with which nanoparticles and nanotubes can be combined with biomolecules in a precisely controlled fashion. For instance, field-effect sensors containing LbL films were produced with poly(dimethyldiallylammonium chloride) (PDMA) immobilized on the gate in conjunction with SnO<sub>2</sub> and SiO<sub>2</sub> nanoparticles.<sup>73</sup> Xu et al. reported a biosensor for detecting lactate with immobilization of MnO<sub>2</sub> nanoparticles alternated with lactate oxidase and PDMA on the gate of an ISFET.<sup>74</sup> The higher sensitivity and improved performance in detecting lactate were attributed to the nanostructured film modifying the gate.<sup>74</sup> One-dimensional nanomaterials including nanowires and nanotubes have been reported as gate-modifying agents for enhanced sensitivity in FET devices. Javey et al. reported an LbL assembly of nanowires (NW) building blocks for NW FETs using Ge/Si core–shell NWs as an approach for 3D multifunctional electronics.<sup>75</sup> A capacitive EIS structure using LbL films of poly(allylamine hydrochloride) (PAH) and PSS was reported by Poghossian et al.<sup>76</sup> Section 4.2.1 will present an overview on the use of carbon nanotubes (CNTs) as a platform for biosensing using FED devices.

**3.4. Spectroscopic Methods.** A variety of spectroscopic methods have been applied for sensing, including direct monitoring of the interaction between an analyte with a sensitive layer, an indicator dye, or a labeled system.<sup>77</sup> In various types of optical spectroscopy, detection is performed by measuring one or more of the optical properties in the sensing device, namely, absorbance, reflectance, fluorescence, and vibrational spectra.<sup>77</sup> Using optical sensors is advantageous because they do not

require a reference signal, suffer no interference from electrical fields, and are amenable to *in vivo* clinical and biological monitoring. Many parameters can thus be monitored, including catalytic activity and analyte concentration.<sup>77</sup> The simplest of such methods is perhaps colorimetry, where color changes in the sample are indicative of the analyte to be detected,<sup>78,79</sup> as exemplified by identification of purpurogallin resulting from oxidation of pyrogallol owing to the enzymatic activity of horseradish peroxidase (HRP) in the presence of hydrogen peroxide. This principle of detection was applied in biosensors containing HRP immobilized either in a phospholipid LB film<sup>78</sup> or in a chitosan matrix in LbL films.<sup>79</sup>

Fluorescence spectroscopy provides a highly sensitive way to detect several molecules of biological interest, including polypeptides and labeled molecules.<sup>77</sup> Another useful method for biosensing is fluorescence resonance energy transfer (FRET),<sup>80</sup> which has been used to investigate molecular interactions due to its sensitivity to distance (typically 10–100 Å). It is based on the radiationless transmission of energy from a donor to an acceptor molecule. The donor may be a dye or chromophore that absorbs energy, whereas the acceptor is a chromophore to which the energy is subsequently transferred, providing the distance-dependent energy transfer. This mechanism in a donor/acceptor pair leads to a reduction in the donor's fluorescence intensity and excited-state lifetime and an increase in the acceptor's emission intensity. Time-resolved FRET immunoassays provide highly sensitive detection of biomarkers in serum samples, with the possible multiplexed clinical diagnostics when quantum dots (QDs) of different colors are used as acceptors.<sup>81</sup>

The use of two-photon or even multiphoton processes in sensing is promising for two main reasons. The first is the deeper penetration in biological tissues provided by the longer light wavelength involved in these processes. The second reason is associated with the possible enhanced spatial resolution, particularly with novel imaging methods. One such example was presented by Jiang et al.,<sup>82</sup> where detection of thrombin on the picomolar level could be reached with a two-photon sensing assay. Their strategy is summarized in the scheme in Figure 8, which shows silver nanoparticles (Ag NPs) coated with a DNA aptamer, referred to as TBA<sub>15</sub>. When light is absorbed by the coated Ag NPs via two-photon processes in the presence of thrombin, the resulting luminescence is enhanced considerably because the specific, strong interaction between thrombin and TBA<sub>15</sub> causes aggregation of the nanoparticles.

The ability to provide fingerprint information on target molecules has been exploited in sensing using vibration spectroscopy techniques. In this context, SERS (surface enhanced Raman spectroscopy) was one of the first methods that made use of "nanostructures" for detection. SERS-based biosensing has grown in different ways, including patterning to create biochips.<sup>83</sup>

**3.5. Surface Plasmon Resonance (SPR).** SPR is exploited in biosensing on the basis of measuring adsorption of a given material on a metallic surface or metal nanoparticle, typically of gold or silver.<sup>84</sup> Such resonance arises from the collective oscillation of electrons excited by light whose photons match the natural frequency of surface electrons. High sensitivity may be achieved because a slight change at the interface, either owing to changes in refractive index or adsorption of molecules, induces changes in the SPR signal. Kara et al.<sup>85</sup> combined molecularly imprinted nanoparticles with SPR for detecting chloramphenicol (CAP) in honey. The nanoparticles were attached onto the SPR

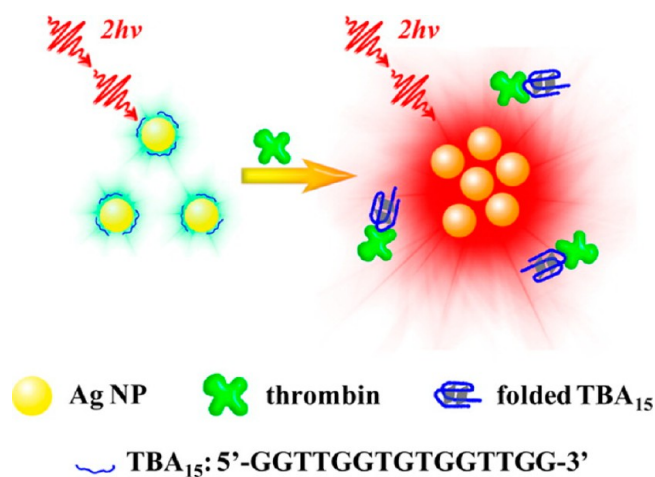


**Figure 8.** Working principle for two-photon sensing of thrombin. Silver nanoparticles (Ag NPs) coated with the DNA aptamer TBA<sub>15</sub> are irradiated, and their photoluminescence is measured. When thrombin is present in the dispersion, its specific interaction with TBA<sub>15</sub> causes the latter to detach from the Ag NPs. Upon aggregation of Ag NPs, the luminescence is increased considerably, which then allows thrombin to be detected optically within the picomolar regime. Reprinted with permission from ref 82. Copyright 2013 American Chemical Society.

nanosensor surface via temperature-controlled evaporation, with which CAP could be recognized selectively.

A summary of the properties and features of the five principles of detection described, as well as their advantages for sensing application in clinical diagnosis, are presented in Table 1.

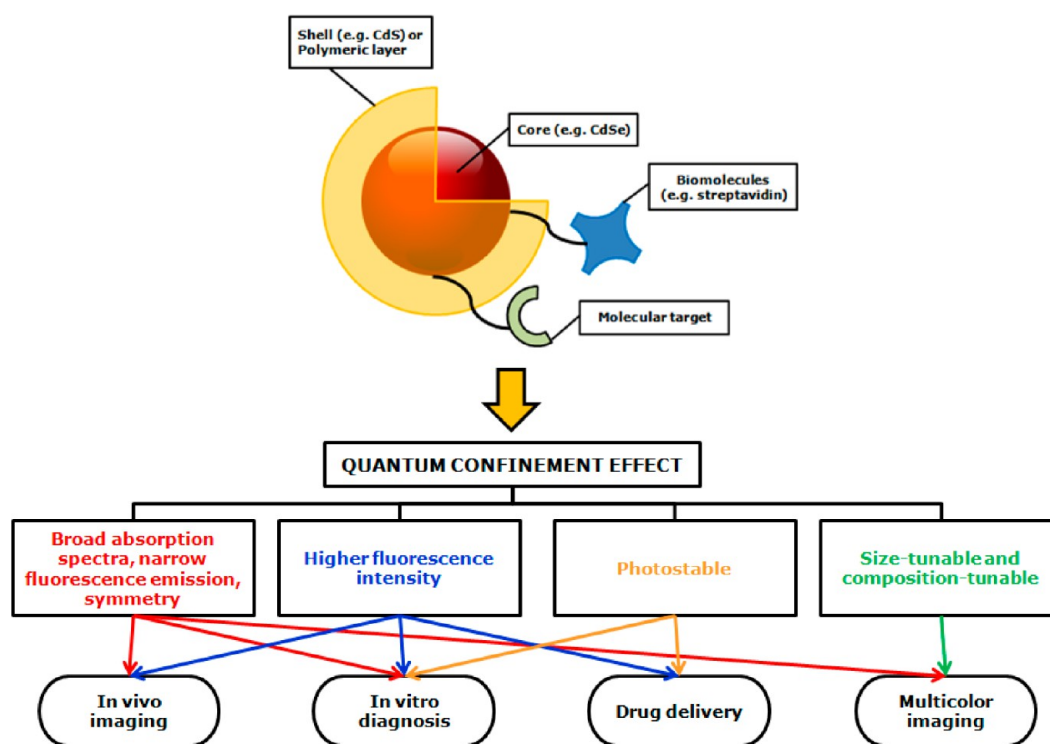
## 4. NANOMATERIALS FOR CLINICAL DIAGNOSIS

**4.1. Quantum Dots.** Semiconductor nanoparticles (or quantum dots (QDs)) exhibit unique optical properties such as size-controlled fluorescence, high quantum yields, narrow fluorescence spectra, and large Stokes shifts in addition to stability against photobleaching. These features are particularly attractive for sensing, as they enable the use of the same materials with size-dependent characteristics as different labels for multiplexed analyses.<sup>80,81</sup> Furthermore, QDs can be functionalized with biomolecules, and such hybrids can probe biocatalytic transformation and recognition events, where detection may be based on FRET or electron transfer (ET). For instance, antibody- or nucleic acid-functionalized QDs of variable sizes have been explored in the multiplexed analysis of pathogens or DNAs.<sup>80,81</sup>

The incorporation of biomolecule–QDs nanostructures into cells may allow for targeting specific intracellular domains, thus enabling the imaging of biotransformation with nanoscale precision. This is one of the reasons why QDs are among the most promising nanomaterials in nanomedicine, not only for diagnostics but also for imaging, targeted drug delivery, and photodynamic therapy for cancer;<sup>80–82,86,87</sup> Figure 9 schematically shows these various possibilities in addition to indicating the relevant features of functionalized QDs. In this specific illustration, CdSe QDs are coated with a shell or polymer layer in addition to molecular targets and biomolecules (e.g., streptavidin) to warrant stability. Several confinement effects may take place, such as broad absorption spectra but narrow fluorescence spectrum, high fluorescence yield, and photostability. Some of the possible applications are also mentioned in Figure 9.

**Table 1. Summary of Properties and Advantages for Each Principle of Detection Applied in Sensing for Clinical Diagnosis**

electrochemical <sup>29</sup>	impedance <sup>70</sup>	field-effect devices <sup>71</sup>	spectroscopy methods <sup>77</sup>	SPR <sup>84,85</sup>
signal based on faradaic or capacitive currents	signal based on changes in resistance or capacitive frequencies	signal based on modulation of current, capacitance, or photocurrent	signal based on characterization of one or more optical properties	signal based on the resonance of photons from light source with sample's surface electrons
charge transfer or transport mechanisms	charge storage or charge transport	electrical surface charge	absorbance, reflectance, fluorescence, and vibrational spectra	electrons excited by light
large variety of methods for sensing	label-free and referenceless detection method	derivate from field-effect transistors (FETs)	large variety of methods for sensing	refractive index or adsorption of molecules for inducing signal detection
diverse options for working electrodes	high sensitivity for liquid and vapors samples	possible integration of sensor arrays in a single chip	no requirement of reference signal, no interference with electrical fields, and amenable to in vivo samples	label-free, real-time measurement, thermodynamic binding parameters
high sensitivity for electroactive samples	suitable for statistical methods analyses	small, low-weight, and low-cost devices	high sensitivity to detect several molecules of biological interest	high sensitivity with slight change at the interface

**Figure 9.** Schematic representation of the diverse applications in which quantum dots have been investigated in cancer diagnosis and treatment. Modified with permission from ref 87. Copyright 2010 Hindawi Publishing Corporation.

Semiconductor QDs are increasingly replacing organic dyes as optical labels for biorecognition events, particularly because the size-controlled luminescence features of QDs facilitate the design of FRET pairs. With the suitable properties of QDs, new possibilities have been created for molecular and cellular imaging as well as for ultrasensitive bioassays and diagnosis of cancer. QDs enable detection of hundreds of cancer biomarkers in blood assays, on cancer tissue biopsies, or as contrast agents for medical imaging. They have the potential to expand in vitro analysis, extending it to cellular, tissue, and whole-body multiplexed cancer biomarker imaging.<sup>80–82,86–92</sup>

Primary tumors detected with QDs include ovarian, breast, prostate, and pancreatic cancer.<sup>87</sup> Wang et al.<sup>93</sup> used QDs with maximum emission wavelength at 605 nm to detect carbohydrate antigen 125 (CA125) in ovarian cancer specimens of different types (fixed cells, tissue sections, and xenograft tumors). The comparison between QDs and fluorescein isothiocyanate (FITC) showed that QD signals were brighter, more specific,

and more stable than those of FITC. Nathwani<sup>94</sup> synthesized biocompatible coated QDs using a chemical route with a natural protein silk fibroin (SF), which were used as fluorescent labels for bioimaging HEYA8 ovarian cancer cells. For breast cancer, diagnosis was performed using QDs in biosensors to detect the human epidermal growth factor receptor (HER2).<sup>95</sup> Multicolor QDs provided quantitative and simultaneous profiling of multiple biomarkers using intact breast cancer cells and clinical specimens. Multicolor bioconjugates were used for simultaneous detection of the five clinically significant tumor markers, including HER2 (QD-HER2), ER (QD-ER), PR (QD-PR), EGFR (QD-EGFR), and mTOR (QD-mTOR), in MCF-7 and BT474 breast cancer cells.<sup>96</sup>

QD probes conjugated with prostate-specific antigen (PSA) were investigated as markers for prostate cancer imaging. Gao et al. achieved sensitive and multicolor fluorescence imaging of cancer cells under in vivo conditions, with metastatic prostate cancer being detected as well.<sup>96</sup> The superior quality of QDs for



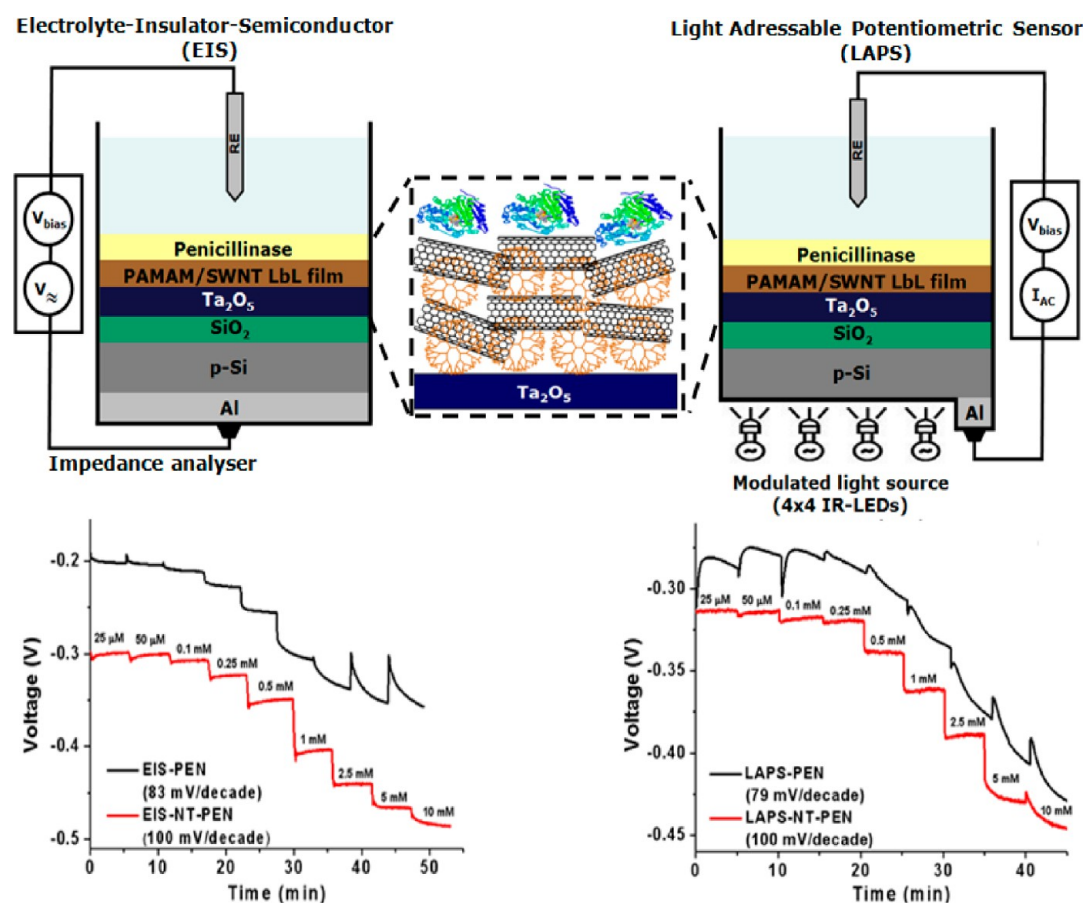


**Figure 10.** (Top) Architectures of a capacitive EIS and a LAPS device, with both being functionalized with a PAMAM/SWNT LbL film and the enzyme penicillinase. (Middle) Zoomed-in view of the LbL film. (Bottom) ConCap and CC responses are shown for different penicillin concentrations in the two types of devices: on the left, for a bare EIS and EIS-NT sensors; on the right, the responses refer to a bare LAPS and a LAPS-NT sensor. Modified with permission from ref 110. Copyright 2010 John Wiley & Sons, Inc.

detecting the androgen receptor (AR) and PSA in prostate cancer cells was also shown by Nie.<sup>97,98</sup> Barua and Rege<sup>99</sup> developed a new method to identify prostate cancer cells with different phenotypes by unconjugated QDs whose trafficking depends on the cell phenotype. Early diagnosis of pancreatic cancer has been achieved with QDs as nanosensors with the help of proteins/peptides directed against overexpressed surface receptors on the cancer cells/tissues.<sup>100</sup> Non-cadmium-based QDs with efficient, nontoxic optical probes for imaging live pancreatic cancer cells were reported by Yong et al.<sup>101</sup> The bioconjugation with pancreatic cancer specific monoclonal antibodies, such as anti-claudin 4, and QDs allowed specific *in vitro* targeting of pancreatic cancer cell lines, demonstrating efficient optical imaging. Further development of QDs might enable their application in detecting and localizing metastasis, measuring molecular targets quantitatively to facilitate targeted therapy, tracking drug delivery, and monitoring the efficacy of therapeutics noninvasively in real time.<sup>120–126</sup>

**4.2. Carbon Materials.** **4.2.1. Carbon Nanotubes.** Carbon nanotubes (CNTs) have been investigated due to their promising mechanical, electrical, and electrochemical properties. Structurally different from other isotropic forms of carbon, CNTs can be formed by the rolling process of graphene sheets.<sup>102</sup> In single-walled carbon nanotubes (SWNTs), every atom is on the surface and therefore even small changes in the environment can cause drastic changes in their electrical properties. Their diameters are comparable to the size of single

molecules (e.g., DNA is 1 nm in size), and they are several micrometers long, thereby providing a convenient interface with micrometer-scale circuitry. Their all-carbon composition also provides a natural match to organic molecules. The chemical functionalization of CNTs<sup>103–105</sup> permits enhancing their solubility and biocompatibility. These features make CNTs promising for sensing.<sup>102,106,107</sup>

Semiconducting SWNTs can be used in FETs that operate at room temperature and under ambient conditions. Their conductivity changes strongly upon physisorption of gases, such as oxygen and ammonia. SWNT-based nanosensors can be fabricated based on a FET layout, where the solid-state gate is replaced by adsorbed molecules that modulate the nanotube conductance (electron donors or electron acceptors).<sup>102,106</sup> There have been two main types of nanodevices including NTFETs. The first uses a single carbon nanotube to act as an electron channel between the source and the drain electrodes. The second type involves a network of carbon nanotubes serving as a collective channel between the source and drain. The analyte–nanotube interaction may have one of two effects. The first effect involves charge transfer from analyte molecules to the carbon nanotubes. In the second type of mechanism, the analyte acts as a scattering potential across the carbon nanotube. The two mechanisms can be distinguished by taking transistor measurements, because if charge transfer occurs, then the threshold voltage will become either more positive (electron withdrawing)

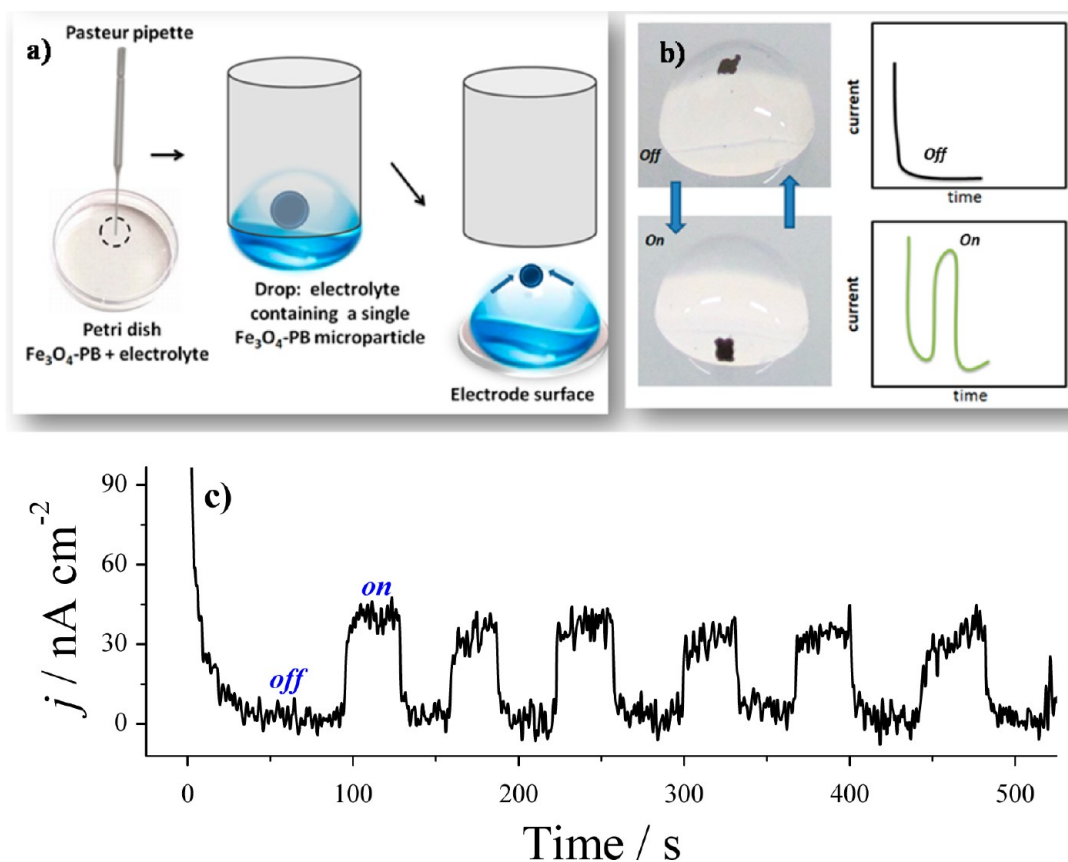


**Figure 11.** (a) Procedure for isolation and manipulation of a single magnetic microparticle. (b) Manipulation of a single  $\text{Fe}_3\text{O}_4$ -PB microparticle in suspension under an external magnetic field. (c) Chronoamperometry experiment showing the magnetic control of the redox process for  $\text{Fe}_3\text{O}_4$ -PB microparticle with the switch-on and -off modes. Applied potential: 0.12 V. Electrolyte: potassium phosphate buffer 0.1 mol  $\text{L}^{-1}$ , pH 7.2. Reprinted with permission from ref 141. Copyright 2013 Elsevier.

or more negative (electron donating). With these features, NTFET devices are useful for detecting biological species.<sup>102,106</sup>

Individual CNTs can also be used in electrochemical single devices,<sup>108</sup> leading to a fast, heterogeneous charge transfer. Electron beam lithography was used to expose a nanometer surface area, and the CNTs functioned as nanoelectrodes with an electrochemical current proportional to the exposed area, reaching 50 pA for a CNT length of 2  $\mu\text{m}$ . Dudin and co-workers<sup>109</sup> employed isolated SWCNTs as templates for electrodeposition of Au, Pd, and Pt metal nanowires (NWs) that can be used for sensing.

CNTs have been incorporated in LbL films used in EIS and LAPS sensors for detecting penicillin G. The capacitive sensor was functionalized with an LbL film containing polyamidoamine (PAMAM) dendrimer and SWNT, with the enzyme penicillinase immobilized atop the film surface.<sup>110,111</sup> For both modified EIS and LAPS devices, the film containing nanotubes enhanced the sensor performance, with higher sensitivity, more stable signal, low drift, and fast response time. The influence of this PAMAM/SWNT-penicillinase film on FED device performance pointed to the importance of film morphology for signal response. The PAMAM/SWNT LbL films acted as highly porous membranes owing to the interpenetration of nanotubes into dendrimer layers, which facilitated ion permeation from enzymatic reactions through the film. Furthermore, the LbL film allowed a stronger, more uniform adsorption of enzymes on the sensor surface.<sup>110,143</sup> Figure 10 depicts the schematic representation of a capacitive EIS structure and a LAPS device functionalized with a

PAMAM/SWNT LbL film and the enzyme penicillinase, as well as their operating principle.

**4.2.2. Graphene.** Graphene is a 2D carbon monolayer arranged in a hexagonal structure with interesting electronic properties,<sup>112</sup> which may be obtained by physical or chemical exfoliation from bulk graphitic materials or with the growth of carbon foils over a substrate. For application in sensing and biosensing,<sup>113</sup> the challenges remain for obtaining high-quality graphene foils with controlled thickness and size,<sup>114</sup> studying the structure of graphene oxide (GO)<sup>115,116</sup> and reduced graphene oxide (rGO),<sup>117</sup> and functionalizing their surface.<sup>118</sup> In spite of these remaining challenges, graphene has been used in many sensing tasks, including for detection of mercury ions,<sup>119</sup> specific genes,<sup>120</sup> and DNA,<sup>121,122</sup> in which the influence of graphene layers onto oxidation of DNA bases<sup>123</sup> has also been explored. Graphene has been found to affect the response of the oxidoreductase enzymes glucose oxidase (GOx),<sup>124</sup> horseradish peroxidase (HRP),<sup>125</sup> cytochrome c,<sup>126</sup> laccase,<sup>127</sup> and bilirubin oxidase.<sup>128</sup> It has also been reported as components in mimetic devices<sup>129</sup> and in FETs and bioFETs where changes in conductivity occur during detection.<sup>130</sup> With nanomanipulation, nanopores<sup>131</sup> and nanochannels<sup>132</sup> were sculpted in graphene using an electron beam, and DNA could be sequenced by passing through them.

**4.3. Nanoparticles.** Many of the works on magnetic nanoparticles dedicated to clinical diagnosis are aimed at enhancing contrast for magnetic resonance imaging. This is the case of iron nanoparticles embedded in hybrid micelles made

with an amphiphilic block copolymer and a peptide amphiphile.<sup>133</sup> In addition to being promising for imaging contrast enhancer, these hybrid micelles could load the anticancer drug doxorubicin, serving therefore for theranostic applications. A fluorescence-based sensing method with gold nanoparticles may provide superior diagnosis capability compared to that of magnetic resonance imaging. Peng et al.<sup>134</sup> detected the activity of a disintegrin and metalloproteinase with thrombospondin motif-4 (ADAMTS-4), which is associated with joint diseases causing cartilage degrading. ADAMTS-4 was detected in the synovial fluid from knee surgery patients by measuring the increase in fluorescence intensity of gold nanoparticle probes obtained with conjugation of the nanoparticles with a FITC-modified ADAMTS-4-specific peptide (DVQEFRGVTAVIR). The high sensitivity and selectivity, with a 3-fold increase in fluorescence reached for only 3.9 pM of ADAMTS-4, made it possible to detect an acute joint injury in a patient whose MR images showed no damage to the cartilage.

Magnetic-controlled bioelectrochemical reactions using a magnetic field were first explored by Willner et al.,<sup>135–137</sup> where magnetite particles ( $\text{Fe}_3\text{O}_4$ ) modified with *N*-(ferrocenylmethyl) aminohexanoic acid were employed to mediate biocatalysis of enzymes.<sup>135</sup> A simple approach with two switchable modes, switch on and switch off, was used to induce the electrochemical current from an enzymatic reaction.<sup>140</sup> The simultaneous control of biocatalytic reactions with two enzymes was reported by Katz et al., with GOx and lactate dehydrogenase (LDH).<sup>138</sup> Liang et al. produced a magneto-controlled bioelectrocatalytic system for glucose oxidation, in which ferrocene was grafted to the thiol-terminated  $\text{Fe}_3\text{O}_4$  nanoparticles via a UV-induced thiolene click reaction.<sup>139</sup>

The micromanipulation of isolated materials such as single magnetic particles has also attracted attention owing to the possible application in diagnostics, as in the case of magnetic control of electrochemical reactions. For instance, Melo and co-workers<sup>141</sup> reported on micromanipulation of a magnetite microparticle modified with the redox mediator Prussian Blue ( $\text{Fe}_3\text{O}_4$ -PB), with a suspension of  $\text{Fe}_3\text{O}_4$ -PB microparticles being collected in a Petri dish using a Pasteur pipette, as indicated in Figure 11a. The second step was the isolation of the microparticle for the electrochemical experiments together with the electrolyte support in a microcapillary (homemade Pasteur pipet) using an optical microscope. Then, the magnetic-switchable electrochemistry study was carried out using an electrochemical microcell with the electrolyte solution containing the magnetic microparticles deposited drop by drop (volume of 20  $\mu\text{L}$ ) on the surface of a screen-printed electrode ( $\text{O} = 4$  mm). The magnetic field was applied to the screen-printed electrode in commutative states with the  $\text{Fe}_3\text{O}_4$ -PB microparticle positioned on the working electrode surface (switch-on state) and outside the electrode surface (switch-off state). The images and current versus time curves for the two states are shown in Figure 11b. These two commutative states provided a switchable control of the electrochemical process of PB, which can be confirmed in the chronoamperometry experiment in Figure 11c. Indeed, an increase of ca. 40  $\text{nA cm}^{-2}$  in the current density was observed between the switch-on and -off states.

Gold nanoparticles (AuNPs) can be conjugated with proteins that have affinity to specific types of cells, thus permitting the diagnosis of various types of diseases.<sup>142</sup> Marangoni et al.<sup>143</sup> fabricated AuNPs stabilized in dendrimers, which were then coated with a layer of jacalin and a fluorescence dye. The main idea was to exploit the differentiation ability by jacalin toward

leukemic cells K562. Their results illustrated in the images in Figure 12 indicate that the AuNPs/jacalin nanoconjugates

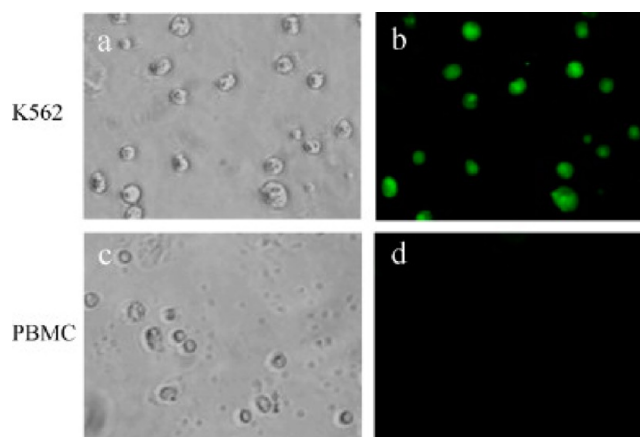


**Figure 12.** Optical and fluorescence microscopy images taken after 3 h of incubation of the AuNPs/jacalin nanoconjugates into cultured K562 leukemia cells (a, b) and PBMCs (c, d). Note the strong adhesion to K562, clearly indicated in the fluorescence image in panel b in contrast to the lack of affinity toward PBMCs in panel d. The magnification in all images was 40X. Reprinted with permission from ref 143. Copyright 2013 Elsevier.

adhered to human K562 leukemia cells, in contrast to the lack of interaction with peripheral blood mononuclear cells (PBMCs) collected from healthy adults. Such high selectivity is promising for diagnosing leukemia as well as for imaging cancer cells.

#### 4.4. Biomolecules as Molecular Recognition Elements.

**4.4.1. Catalytic Antibodies.** Catalytic antibodies, also known as abzymes or catmabs, are monoclonal antibodies with catalytic activity. Although found in humans with autoimmune diseases, such as lupus, they are normally constructed artificially. These antibodies are candidates for biotechnology, especially for ester hydrolysis or for manipulating nucleic acids, where properties of enzymes and antibodies are combined. Enzymes provide a reaction mechanism with a lower value of activation energy to reach the transition state than for the corresponding non-catalyzed reaction. Therefore, antibodies able to stabilize the energy of an intermediate state, chemically changing the antigen after the process, behave as enzymes. They can be used in biosensors to identify chemical and biological agents, in addition to therapeutic applications.

In sensing and diagnosis, catalytic antibodies have been used to hydrolyze benzoyl ester from cocaine<sup>144</sup> in an approach to destroy cocaine prior to its absorption into the brain by depleting and inactivating available antibodies. Catalytic antibodies have also served for the oxidative degradation of nicotine<sup>145</sup> and reactive immunization to activate prodrug.<sup>146</sup> Mu et al.<sup>147</sup> obtained phage antibodies with glutathione peroxidase (GPX)-binding site by enzyme-linked immunosorbent assay (ELISA) analysis. They used four rounds of selection against three haptens based on esters and then tested the device as a sensor using SPR. A gold layer was modified by dithiodiglycolic acid (DDA), and the haptens were attached to DDA by self-assembling to form a biosensor membrane that interacted specifically with the corresponding antibodies. It was claimed that the GPX activity was more rapid and simple than conventional ELISA analysis.

Blackburn et al.<sup>148</sup> developed a prototype potentiometric biosensor in which a micro-pH electrode was modified with a catalytic antibody that catalyzes the hydrolysis of phenyl acetate,

producing hydrogen ions to be monitored by the electrode. Yang et al.<sup>149</sup> showed that ibuprofen ester could be monitored by catalytic antibodies in water-miscible organic solvents. The hydrolysis with dimethylformamide had twice the catalytic efficiency for the buffer solution and therefore catalytic antibodies may act as the molecular recognition element in biosensors with tailored properties.

**4.4.2. DNA, RNA, and Nucleic Acids.** Manipulation of antibodies may be problematic in diagnosis owing to stability, which prompted researchers to consider nucleic acid aptamers as alternatives for molecular recognition.<sup>150</sup> These aptamers are made from short strands of DNA or RNA, e.g., with the DNA double helix being broken to form a single-strand DNA (ssDNA) (e.g., under higher pH and temperature).<sup>151</sup> The reannealing of DNA structure forming the double helix through hybridization is the basis for specific gene identification in biosensing devices.<sup>151,152</sup> Alternatively, nucleic acid can be immobilized onto a solid surface for recognizing DNA with a specific sequence.<sup>153</sup> The first DNA biosensor was published in 1993 using a reversible electroactive cobalt complex for voltammetric detection of covalently immobilized DNA.<sup>154</sup> Since then, other principles of detection have been used, including optical,<sup>155</sup> piezoelectric,<sup>156</sup> electrical,<sup>157</sup> and electrochemical measurements.<sup>158,159</sup>

DNA biosensors have been obtained with several methods of immobilization<sup>160,161</sup> and in conjunction with other nanomaterials.<sup>121,162,163</sup> In electrochemical sensors, the signal was maximized with silver nanoparticles (AgNPs)<sup>164,165</sup> or gold nanoparticles (AuNPs),<sup>163,166</sup> especially in cases where AuNPs were capable of improving DNA loading.<sup>167</sup> AuNPs could be coated with ferrocene and were selective for oligonucleotides and polynucleotides.<sup>168</sup> Other nanomaterials used in DNA biosensors are CNTs and graphene.<sup>169</sup> Electrodes were coated with functionalized multiwalled carbon nanotubes (MWCNTs) to enhance the kinetics of charge transfer between the electrode and daunomicyn to detect the complementary oligonucleotide with concentrations down to  $1 \times 10^{-10}$  mol L<sup>-1</sup>.<sup>162</sup> Metallic nanoparticles and CNTs have also been combined in DNA biosensors, in some cases in a polymer matrix.<sup>164,165,170</sup>

**4.4.3. Enzymes and Other Proteins.** Enzymes have been applied for many years in clinical diagnosis. Glucose oxidase (GOx) was one of the first to be used, perhaps because glucose concentration is a crucial indicator in endocrine metabolic disorders, including diabetes. Under normal physiological conditions, glucose concentration fluctuates within  $110 \pm 25$  mg dL<sup>-1</sup> (around 6  $\mu$ M), whereas diabetics may reach 360 mg dL<sup>-1</sup> (20  $\mu$ M) or higher.<sup>171</sup> Biosensors functioning for these ranges are important to control glucose concentration in the blood of patients, both in hospitals as well as in their homes. The first widely commercialized biosensor was for glucose detection.<sup>172</sup> Peroxidases are also extensively used in biosensors,<sup>173</sup> including in cases where a more sophisticated molecular architecture had to be created out of nanomaterials. For instance, a magnetic-controlled noncompetitive enzyme-linked voltammetric immunoassay was proposed based on the immunoaffinity reaction between horseradish peroxidase immobilized with carcinoembryonic antigen functionalized with magnetic CoFe<sub>2</sub>SO<sub>4</sub> nanoparticles.<sup>174</sup> With this architecture, the active center of the enzyme was partially inhibited by the antigen-antibody complex, which decreased the level of peroxide reduction.

The importance of molecular architecture has been shown repeatedly in biosensors made with enzymes immobilized in

nanostructured films.<sup>175</sup> Such biosensors could be made from cholesterol oxidase<sup>176,177</sup> to detect cholesterol, from uricase<sup>178,179</sup> to detect uric acid, from urease to detect urea,<sup>39,180–182</sup> and from organophosphorous hydrolase (OPH) bonded to a fluorescein probe to detect paraoxon. OPH was also used for sensing paraoxon interacting with LbL films of chitosan<sup>183</sup> and for antibodies interacting with LB films of viologen and protein-A.<sup>184</sup> In biosensors produced with LbL films, the number of enzyme layers can increase the sensitivity owing to an increased amount deposited.<sup>185,186</sup> In other instances, it is better to keep the enzyme only on the topmost layer because the main reactions occur on the surface.<sup>47,187</sup> Also worth mentioning is a nanoscale protein chip prepared with an etched polystyrene (PS) template, immobilized as LB films, used for an immunoassay exploring SERS spectra.<sup>188</sup>

## 5. IMPLANTABLE AND MULTIPURPOSE BIOSENSORS: TOWARD SMART DEVICES

The possibility of real-time tracking inside the human body has opened the way for a large number of applications, which include implantable biosensors that may serve not only for diagnostics but also as component of a therapeutic strategy based on controlled drug delivery. This is what has been referred to as smart devices in the literature, which may offer continuous diagnosis, prognosis, and therapeutic management.<sup>189</sup> The development of these smart devices relies heavily on nanomaterials, as will be clear in the examples below.

Gastrointestinal bleeding could be monitored *in vivo* in real time in pig models using wireless endoscopy,<sup>190</sup> as biosensors were able to detect all events of acute bleeding and a text message could be sent to the desired phone number. An implantable real-time sensor able to monitor pressure in the body was obtained with a soft magnetic material and a permanent magnet.<sup>191</sup> When exposed to a low-frequency ac magnetic field, the soft magnetic material generated secondary magnetic fields, based on which stress/strain and pressure sensors could be developed. Such sensing may be useful for monitoring biomedical implants. Another important issue in this monitoring is related to ensuring the proper functioning of the sensors, as exemplified in implantable biosensors to detect carbohydrates where a statistical method was used to locate causes of sensor drift.<sup>192</sup>

Also named smart devices are those operating in multiplex platforms, as in the array shown in Figure 13 for detecting pathogens and cancer markers.<sup>193–195</sup> The resolution of subtle electrochemical variations is associated with DNA substrate and surface morphology, for which multiplexed analysis leads to more reliable statistics as well as decreased surface variability and background contribution. With the array in Figure 13, one may investigate DNA-mediated reduction of metalloproteins.<sup>194</sup>

The same principle of multiplex analysis was applied to detect human DNA methyltransferase<sup>193</sup> by exploiting the finding that aberrant methylation by methyltransferases enzymes is associated with cancer. Barton and co-workers<sup>193</sup> described an electrochemical assay detecting methyltransferase activity with DNA-modified electrodes (multiplexed electrodes), as shown in Figure 14.

The creation of smart devices depends on convergence of various technologies associated with sensing, actuating, controlled drug delivery, wearable devices, mobile energy sources, data analysis, robotics, and wireless communications, just to mention a few. The result from such convergence can be rewarding in terms of offering minimally intrusive individualized health services<sup>196</sup> in addition to possibly improving the

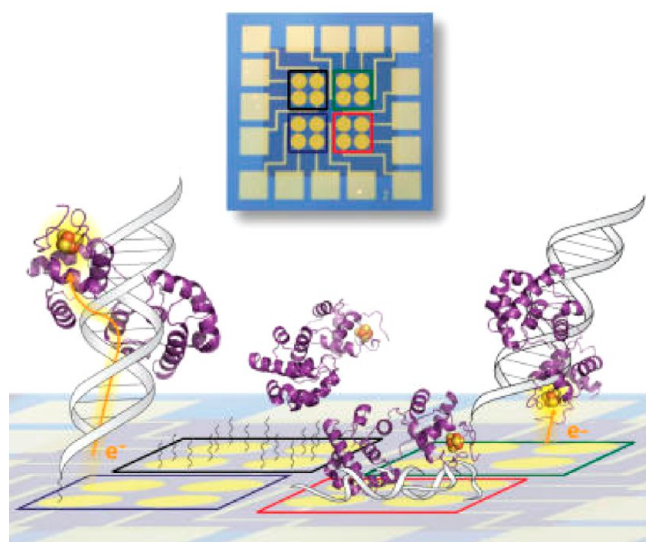


**Figure 13.** (Top) Multiplex device with 16 electrodes divided into four quadrants. In each electrode on the Au surface a different experimental condition can be used for investigating metalloprotein electrochemistry, and this is illustrated schematically (Bottom) where distinct DNA-bound protein systems are shown. Reprinted with permission from ref 194. Copyright 2013 American Chemical Society.

performance of the human body and repairing vital biological functions.

## 6. STATISTICAL AND COMPUTATIONAL METHODS FOR DATA ANALYSIS

The concept of expert systems for clinical diagnosis has been introduced decades ago.<sup>197</sup> These expert systems are basically aimed at emulating what doctors do in their diagnosis but with enhanced capability provided by a computational system that takes advantage of two features: the ability to handle a much

larger amount of data and the ability to store much more information about diseases and symptoms. The prominence achieved in recent years by the challenges associated with the so-called “big data” or e-Science (or data-intensive discovery)<sup>198</sup> highlights the promise held by expert systems that could now benefit from a much larger computational capacity than they could decades ago. The modules for such a system should comprise (i) modules dedicated to storing various types of data, (ii) modules for preprocessing and processing data, and (iii) the diagnosis modules per se. In the first type of module, input data may come from clinical exams, medical images, clinical reports, history of the patient, and from other patients.<sup>199</sup> The preprocessing and processing modules must contain statistical and computational tools for cleaning and formatting the data, data mining, and visualization.<sup>200</sup> The modules for diagnosis per se may be based on machine learning methods<sup>201</sup> and perhaps include an interface in natural language provided by a language generation system.<sup>202</sup> The computational diagnosis system must be implemented so as to acquire (and learn) new information from the present exams and analysis.

While most of the modules mentioned above are not related to nanomaterials, it is clear that the expert system will rely on data from sensors, biosensors, and imaging devices, many of which may be similar to those discussed in this review. Moreover, the amount of data generated in measurements with state-of-the-art equipment is already huge and therefore statistical and computational methods will soon be mandatory for data analysis.<sup>203</sup> This is particularly true for clinical diagnosis owing to the variability inherent in biological samples, especially when imaging is involved.

In a visionary paper in 2004, Dermot Diamond<sup>204</sup> proposed ways to connect the molecular world to the digital world, in which analytical scientists would play an important role in providing the gateway. Such connection would rely on Internet-scale sensing and control through wireless sensor networks for chemo-/biosensing.<sup>205</sup> Figure 15 illustrates such concepts with a

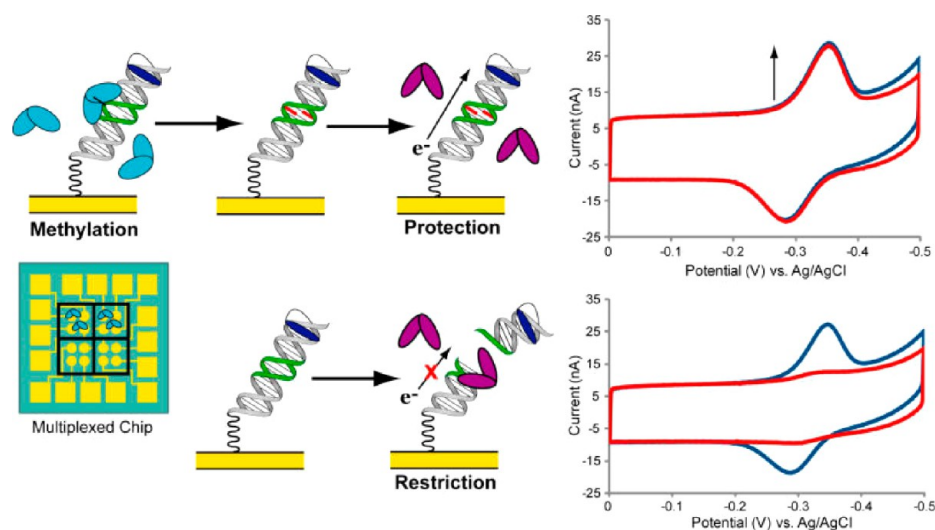


**Figure 14.** (Bottom left) Multiplexed chip used to distinguish between DNA-modified electrodes protected from cutting and those where a restriction enzyme cuts DNA. The electrodes had recognition sites of methyltransferase and restriction enzyme (green section of DNA). (Top left) The electrodes are methylated (red DNA bases) in the presence of active methyltransferases. Because DNA was protected from cutting, the cyclic voltammograms were essentially the same, with a signal-on result before (blue trace) and after (red trace) the treatment with the active methyltransferase. (Bottom right) A signal-off result obtained because of the treatment with the restriction enzyme in the absence of active methyltransferases (bottom left). In the latter case, the DNA is cut by the restriction enzyme because it remains unmethylated. Reprinted with permission from ref 193. Copyright 2013 American Chemical Society.

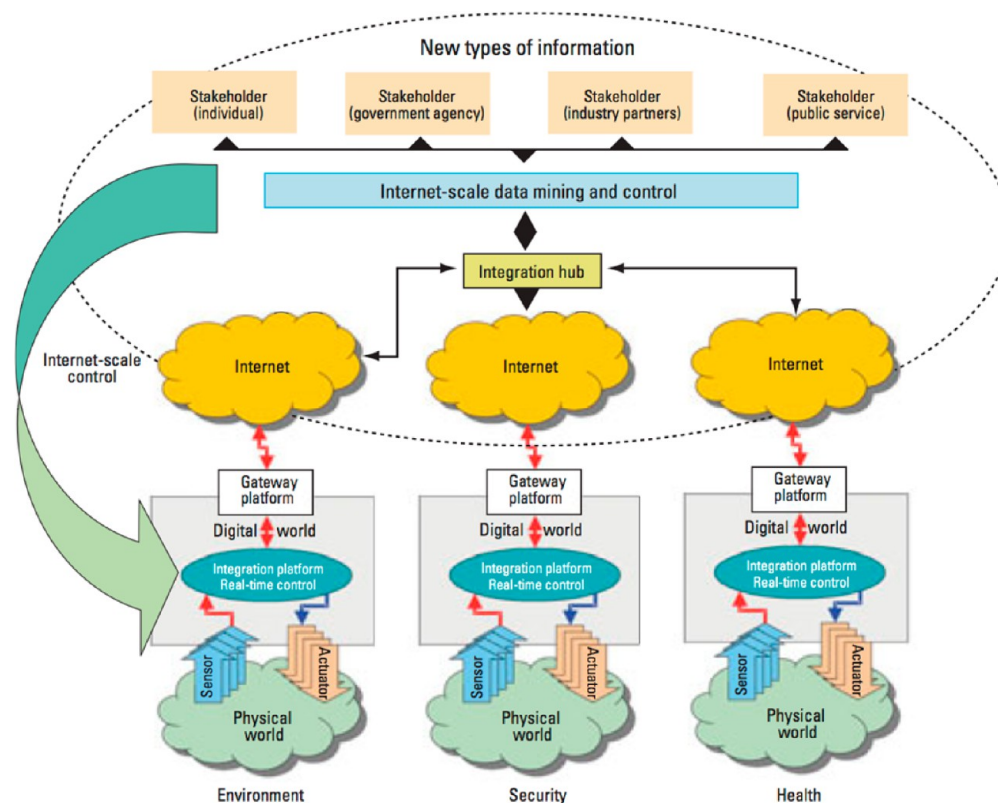


**Figure 15.** Flowchart with a proposed strategy to connect the molecular world, represented by the access to sensing devices data, to the digital world. Data from millions of sensing devices would be input into the system by various types of stakeholders, which would be mined with distinct computational methods. Also envisaged are control systems to perform specific tasks as feedback to the input sensing data; therefore, the whole system should also contain actuators. This so-called Internet-scale control can be used in the physical world across many applications, three of which are represented in the figure. Reprinted with permission from ref 204. Copyright 2004 American Chemical Society.

flowchart indicating that new types of information would be input into the whole system by various stakeholders, from individuals to industry partners and government agencies. Millions of sensing devices would provide data for applications that may range from monitoring the environment to health, including clinical diagnosis. The heart of the proposed strategy is data mining and control via the Internet, which would amount to an expert system similar to that described in the paragraph above.

The computational methods for such endeavors encompass artificial neural networks,<sup>206</sup> visualization techniques,<sup>207,208</sup> and machine learning techniques.<sup>209</sup> For instance, the level of glucose in diabetic human subjects has been monitored by measuring the electric current resulting from the transport of glucose interacting with glucose oxidase in a hydrogel placed on the skin surface.<sup>210</sup> Owing to the complexity of the signal, the glucose concentration in the blood could be obtained only with the machine learning expectation maximization algorithm.<sup>210</sup> Another field explored in classification tasks is pattern recognition using methods from signal processing, such as fast Fourier transform (FFT), as illustrated recently in human-machine interfacing where muscle motion is tracked with a sensor array.<sup>211</sup> Similarly, imaging of a patterned chip from a cell phone camera has been used for point-of-care diagnosis.<sup>212</sup>

In this review, we emphasize the importance of these methods for biosensing, with examples from the use of information visualization (for a review, see ref 203). In many respects, such use resembles applications from chemometrics<sup>213</sup> and multivariate data analysis.<sup>214</sup> In particular, multidimensional projections have already been proven to be useful for biosensing, with

data elements from a high-dimensional space being mapped on a 2D or 3D plot. In these projections, a measure of similarity/dissimilarity is defined by a distance function in the high-dimensional data space. These techniques are related to dimensionality reduction and multidimensional scaling (MDS)<sup>215</sup> approaches, such as principal component analysis (PCA)<sup>216</sup> and classical scaling.<sup>215</sup> A successful distance<sup>217</sup> function for biosensing has been the so-called interactive document map (IDMAP).<sup>217</sup> It differs from PCA and MDS because the placement of the data elements is optimized using a cost function that tries to minimize the error inherent in projecting the data onto a low-dimension space, with the aim of placing similar samples in the original space close to each other in the projected space. In IDMAP, the nonlinear cost function is defined as

$$S_{\text{IDMAP}} = \frac{\delta(x_i, x_j) - \delta_{\min}}{\delta_{\max} - \delta_{\min}} - d(y_i, y_j)$$

where  $\delta_{\min}$  and  $\delta_{\max}$  are the minimum and maximum distances between the samples, respectively.

Two examples are illustrated here. In the first, impedance spectroscopy data were projected using the IDMAP<sup>218</sup> technique. The data were obtained by immersing a biosensor made with an antigenic peptide, 24-3, which is capable of molecular recognition toward anti-p24 antibodies (representing HIV), where the peptide was immobilized in liposomes in LbL films.<sup>218</sup> Each point in the projection corresponds to the spectrum for the real component of the electrical impedance, from 1 Hz to 1 MHz. The projection indicated clear distinction

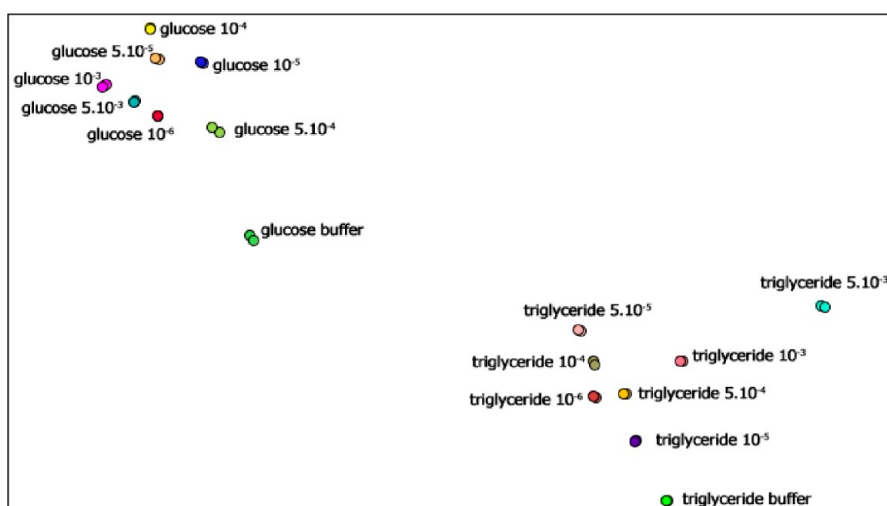


**Figure 16.** IDMAP plot for the combined capacitance and loss data for with two sensing units. The latter were fabricated by adsorbing LbL films onto interdigitated gold electrodes. One of the units contained LbL films with alternating layers of poly(allylamine hydrochloride) (PAH)/glucose oxidase (GOx), whereas the other had a PAH/lipase LbL film. Each point in the plot represents the spectrum with 10 selected frequencies, rather than the whole spectrum. Reprinted with permission from ref 219. Copyright 2012 Elsevier.

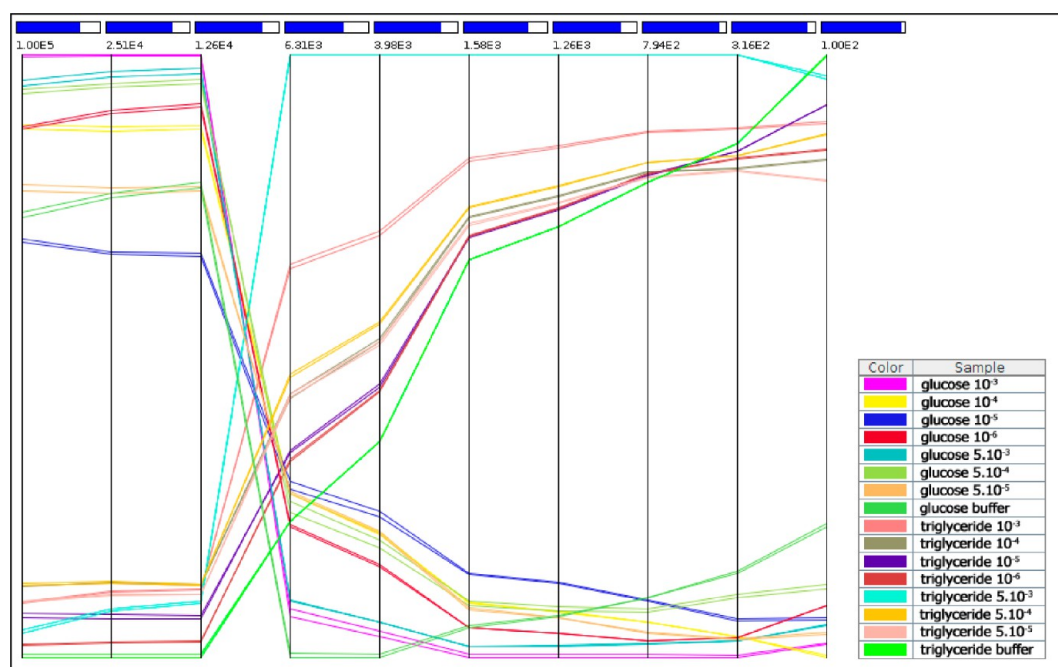


**Figure 17.** Use of the parallel coordinates technique to plot the capacitance and loss data for the two sensing units mentioned in Figure 16. Only the data of the 10 best frequencies are shown. These frequencies are marked with blue boxes to indicate that they were useful for distinction, according to their silhouette coefficient. Reprinted with permission ref 219. Copyright 2012 Elsevier.

between samples with different anti-p24 antibody concentrations, whereas the sample containing the nonspecific anti-HCV antibody could not be distinguished from the PBS buffer.

In the second example, samples containing varied concentrations of glucose or triglycerides could be clearly distinguished, as indicated in the IDMAP plot of Figure 16. Motivation for this work came from the interference of one of these analytes in the determination of the other in real samples for clinical diagnosis. Each point in the projection corresponds to the spectrum from 1 Hz to 1 MHz, as mentioned for the example above. There are, however, two important differences. In the optimization procedure for reaching the best distinguishing ability, Moraes et al.<sup>219</sup> found that a combination of capacitance and loss data

was more efficient than simply using the real or imaginary component of the electrical impedance. The second, and most important, difference is that not all of the values for all frequencies were considered because a feature selection approach was used.

Optimization via feature selection was performed, in which only the 10 best frequencies were used, as follows: A technique referred to as parallel coordinates was employed, where an axis is associated with each data attribute and used to map its range, with the axes arranged in parallel on the plane. A polyline represents a data instance that will cross the attribute axes according to the value of the corresponding attribute. Figure 17 shows a parallel coordinates plot in which the  $x$  axis represents

the frequency, whereas the  $y$  axis brings the normalized capacitance and loss values. A visual inspection confirms that the frequencies were suitable for distinction of the various samples indicated in the inset.

The suitable frequencies in Figure 17 were marked with blue boxes to mean that the silhouette coefficient<sup>203</sup> that assesses the quality of a data cluster is high. The silhouette metric varies between  $-1$  and  $1$ , where higher values indicate better quality. The silhouette coefficient is given by

$$S_c = \frac{1}{n} \sum_{i=1}^n \frac{(b_i - a_i)}{\max(a_i, b_i)}$$

where  $a_i$  is the average distance between the  $i$ th data point and all other points of the same cluster and  $b_i$  is the minimum distance between the  $i$ th data point and the points from the other clusters. The blue boxes mean that all the frequencies selected have a high  $S_c$ , close to  $1$ . Because scanning the whole data space of cluster silhouettes is time-consuming, Moraes et al.<sup>219</sup> used a genetic algorithm to automatically identify the best frequencies for distinction.

The methods from information visualization and artificial intelligence illustrated in the two examples above are completely generic and may be extended to any type of data. Indeed, information visualization has been explored to treat electrochemical data from field-effect devices<sup>220</sup> and surface-enhanced Raman scattering spectra for single-molecule detection.<sup>221</sup> All of these examples dealt with localized, lab-based methods, for which the use of computational methods was already useful. Much more can be expected if such methods are employed within a fully fledged expert system for clinical diagnosis, for instance, to apply therapies based on remotely monitored disease markers. Then, various other issues will have to be addressed.<sup>204</sup> Of crucial importance are the ethical and moral issues related to the access of the data stored by individuals, companies, and government agencies. Although these may be hard-to-solve problems, the implication of such systems is clear. As Dermot Diamond puts it, "analytical science will be at the center of the next communications revolution".

## 7. CONCLUDING REMARKS

Advances in materials science, biotechnology, and data processing have changed the landscape of clinical diagnosis in recent years. Generally, advances in different areas appear to be disconnected, especially because the issues addressed for improving diagnosis belong to very distinct areas. Diagnosis is obviously related to medicine, but the methodologies on which it is based are created by developers from an ever increasing number of fields. In this review, we focused primarily on the importance of materials science, particularly with nanomaterials, also including a hint of the convergence of technologies that may take over with the use of computational methods. The emphasis, while describing the use of nanomaterials for biosensing, was placed on the possible control of molecular architectures that is now available with film fabrication methods and functionalization of surfaces. Of particular relevance in this regard is the understanding of the way nanomaterials, including naturally occurring biomolecules, function in the nanostructures with which the biosensors are made. We did not aim at a full coverage of the literature, for, in addition to being a daunting task, the reader would likely get lost with an exceedingly long list of nanomaterials that are now used in clinical diagnosis. Instead, we tried to highlight the most important classes while also

connecting the contributions in the literature with the variety of principles of detection for biosensing.

As for the convergence of technologies, we dedicated a whole section to the prospects of the use of data-intensive discovery and related methods for clinical diagnosis. This is actually a field that may develop in so many different ways in the near future. More than enhancing the capabilities for diagnosis, with these methods and networks of sensors and biosensors, one may envisage the digital world being able to control the real world on the molecular level, as has been anticipated by Diamond.<sup>205</sup>

## AUTHOR INFORMATION

### Corresponding Author

\*E-mail: chu@ifsc.usp.br. Tel: +55 16 33739825. Fax: +55 1633715365.

### Notes

The authors declare no competing financial interest.

## ACKNOWLEDGMENTS

This work was supported by FAPESP, CNPq, CAPES, and nBioNet network (Brazil).

## REFERENCES

- (1) Rolfe, P. Micro- and Nanosensors for Medical and Biological Measurement. *Sens. Mater.* **2012**, *24*, 275–302.
- (2) Famulok, M.; Mayer, G. Aptamer Modules as Sensors and Detectors. *Acc. Chem. Res.* **2011**, *44*, 1349–1358.
- (3) Palermo, V.; Palma, M.; Samori, P. Electronic Characterization of Organic Thin Films by Kelvin Probe Force Microscopy. *Adv. Mater.* **2006**, *18*, 145–164.
- (4) Decher, G. Fuzzy Nanoassemblies: Toward Layered Polymeric Multicomposites. *Science* **1997**, *277*, 1232–1237.
- (5) Huh, Y.-M.; Jun, Y.-w.; Song, H.-T.; Kim, S.; Choi, J.-s.; Lee, J.-H.; Yoon, S.; Kim, K.-S.; Shin, J.-S.; Suh, J.-S.; Cheon, J. In Vivo Magnetic Resonance Detection of Cancer by Using Multifunctional Magnetic Nanocrystals. *J. Am. Chem. Soc.* **2005**, *127*, 12387–12391.
- (6) Yan, Y.; Bjonmalm, M.; Caruso, F. Assembly of Layer-by-Layer Particles and Their Interactions with Biological Systems. *Chem. Mater.* **2014**, *26*, 452–460.
- (7) Such, G. K.; Johnston, A. P. R.; Caruso, F. Engineered Hydrogen-Bonded Polymer Multilayers: From Assembly to Biomedical Applications. *Chem. Soc. Rev.* **2011**, *40*, 19–29.
- (8) Takahashi, S.; Sato, K.; Anzai, J. Layer-by-layer Construction of Protein Architectures through Avidin–Biotin and Lectin–Sugar Interactions for Biosensor Applications. *Anal. Bioanal. Chem.* **2012**, *402*, 1749–1758.
- (9) Vannoy, C. H.; Tavares, A. J.; Noor, M. O.; Uddayasankar, U.; Krull, U. J. Biosensing with Quantum Dots: A Microfluidic Approach. *Sensors* **2011**, *11*, 9732–9763.
- (10) Ariga, K.; Ito, H.; Hill, J. P.; Tsukube, H. Molecular Recognition: From Solution Science to Nano/Materials Technology. *Chem. Soc. Rev.* **2012**, *41*, 5800–5835.
- (11) Zasadzinski, J. A.; Viswanathan, R.; Madsen, L.; Garnæs, J.; Schwartz, D. K. Langmuir–Blodgett Films. *Science* **1994**, *263*, 1726–1733.
- (12) Ariga, K.; Yamauchi, Y.; Mori, T.; Hill, J. P. 25th Anniversary Article: What Can Be Done with the Langmuir–Blodgett Method? Recent Developments and Its Critical Role in Materials Science. *Adv. Mater.* **2013**, *25*, 6477–6512.
- (13) Decher, G.; Hong, J. D.; Schmitt, J. Buildup of Ultrathin Multilayer Films by a Self-Assembly Process 0.3. Consecutively Alternating Adsorption of Anionic and Cationic Polyelectrolytes on Charged Surfaces. *Thin Solid Films* **1992**, *210*, 831–835.
- (14) Ariga, K.; Yamauchi, Y.; Rydzek, G.; Ji, Q. M.; Yonamine, Y.; Wu, K. C. W.; Hill, J. P. Layer-by-layer Nanoarchitectonics: Invention, Innovation, and Evolution. *Chem. Lett.* **2014**, *43*, 36–68.



- (15) Love, J. C.; Estroff, L. A.; Kriebel, J. K.; Nuzzo, R. G.; Whitesides, G. M. Self-Assembled Monolayers of Thiolates on Metals as a Form of Nanotechnology. *Chem. Rev.* **2005**, *105*, 1103–1169.
- (16) Srivastava, S.; Kotov, N. A. Composite Layer-by-Layer (LBL) Assembly with Inorganic Nanoparticles and Nanowires. *Acc. Chem. Res.* **2008**, *41*, 1831–1841.
- (17) Lu, F.; Tian, Y.; Liu, M.; Su, D.; Zhang, H.; Govorov, A. O.; Gang, O. Discrete Nanocubes as Plasmonic Reporters of Molecular Chirality. *Nano Lett.* **2013**, *13*, 3145–3151.
- (18) Zhang, X. X.; Han, X. F.; Wu, F. G.; Jasensky, J.; Chen, Z. Nano-Bio Interfaces Probed by Advanced Optical Spectroscopy: From Model System Studies to Optical Biosensors. *Chin. Sci. Bull.* **2013**, *58*, 2537–2556.
- (19) Caseli, L.; Gruber, J.; Li, R. W. C.; Peres, L. O. Investigation of the Conformational Changes of a Conducting Polymer in Gas Sensor Active Layers by Means of Polarization-Modulation Infrared Reflection Absorption Spectroscopy (PM-IRRAS). *Langmuir* **2013**, *29*, 2640–2645.
- (20) Niu, Y.; Jin, G. Protein Microarray Biosensors Based on Imaging Ellipsometry Techniques and Their Applications. *Protein Cell* **2011**, *2*, 445–455.
- (21) Hinrichs, K.; Gensch, M.; Esser, N.; Schade, U.; Rappich, J.; Kroning, S.; Portwich, M.; Volkmer, R. Analysis of Biosensors by Chemically Specific Optical Techniques. Chemiluminescence-imaging and Infrared Spectroscopic Mapping Ellipsometry. *Anal. Bioanal. Chem.* **2007**, *387*, 1823–1829.
- (22) Elovsson, K.; Pei, Z. C.; Aastrup, T. Cell-Based Biosensors: A Quartz Crystal Microbalance Approach to Membrane Protein Interaction Studies. *Am. Lab.* **2011**, *43*, 26–27.
- (23) Lee, S.; Kim, Y. I.; Kim, K. B. Comparative Study of Binding Constants from Love Wave Surface Acoustic Wave and Surface Plasmon Resonance Biosensors Using Kinetic Analysis. *J. Nanosci. Nanotechnol.* **2013**, *13*, 7319–7324.
- (24) Manickam, A.; Johnson, C. A.; Kavusi, S.; Hassibi, A. Interface Design for CMOS-Integrated Electrochemical Impedance Spectroscopy (EIS) Biosensors. *Sensors* **2012**, *12*, 14467–14488.
- (25) Marzo, F. F.; Pierna, A. R.; Barranco, J.; Lorenzo, A.; Barroso, J.; Garcia, J. A.; Perez, A. Determination of Trace Metal Release During Corrosion Characterization of FeCo-based Amorphous Metallic Materials by Stripping Voltammetry. New Materials for GMI biosensors. *J. Non-Cryst. Solids* **2008**, *354*, 5169–5171.
- (26) Xiong, M.; Gu, B.; Zhang, J. D.; Xu, J. J.; Chen, H. Y.; Zhong, H. Glucose Microfluidic Biosensors Based on Reversible Enzyme Immobilization on Photopatterned Stimuli-Responsive Polymer. *Biosens. Bioelectron.* **2013**, *50*, 229–234.
- (27) Wang, J. L.; Chen, G. H.; Jiang, H.; Li, Z. Y.; Wang, X. M. Advances in Nano-Scaled Biosensors for Biomedical Applications. *Analyst* **2013**, *138*, 4427–4435.
- (28) Moraes, M. L.; Maki, R. M.; Paulovich, F. V.; Rodrigues, U. P.; de Oliveira, M. C. F.; Riul, A.; de Souza, N. C.; Ferreira, M.; Gomes, H. L.; Oliveira, O. N., Jr. Strategies to Optimize Biosensors Based on Impedance Spectroscopy to Detect Phytic Acid Using Layer-by-Layer Films. *Anal. Chem.* **2010**, *82*, 3239–3246.
- (29) Iost, R. M.; Crespilho, F. N. Layer-by-layer Self-assembly and Electrochemistry: Applications in Biosensing and Bioelectronics. *Biosens. Bioelectron.* **2012**, *31*, 1–10.
- (30) Iost, R. M.; Madurro, J. M.; Brito-Madurro, A. G.; Nantes, I. L.; Caseli, L.; Crespilho, F. N. Strategies of Nano-Manipulation for Application in Electrochemical Biosensors. *Int. J. Electrochem. Sci.* **2011**, *6*, 2965–2997.
- (31) Blodgett, K. B. Monomolecular Films of Fatty Acids on Glass. *J. Am. Chem. Soc.* **1934**, *56*, 495–495.
- (32) Pichot, R.; Watson, R. L.; Norton, I. T. Phospholipids at the Interface: Current Trends and Challenges. *Int. J. Mol. Sci.* **2013**, *14*, 11767–11794.
- (33) Acharaya, S.; Shundo, A.; Hill, J. P.; Ariga, K. Langmuir Films of Unusual Components. *J. Nanosci. Nanotechnol.* **2009**, *9*, 3–18.
- (34) Hasmonay, H.; Caillaud, M.; Dupeyrat, M. Langmuir–Blodgett Multilayers of Phosphatidic-Acid and Mixed Phospholipids. *Biochem. Biophys. Res. Commun.* **1979**, *89*, 338–344.
- (35) Sriyudthsak, M.; Yamagishi, H.; Moriizumi, T. Enzyme-Immobilized Langmuir–Blodgett Film for a Biosensor. *Thin Solid Films* **1988**, *160*, 463–469.
- (36) Savitsky, A. P.; Dubrovsky, T. B.; Demcheva, M. V.; Mantrova, E. Y.; Savransky, V. V.; Belovolova, L. V. Fluorescent and Phosphorescent Study of Langmuir–Blodgett Antibody Films for Application to Optical Immunosensors. *Proc. SPIE* **1993**, *1885*, 168–176.
- (37) Wang, F.; Xu, Y.; Wang, L.; Lu, K.; Ye, B. X. Immobilization of DNA on a Glassy Carbon Electrode Based on Langmuir–Blodgett Technique: Application to the Detection of Epinephrine. *J. Solid State Electrochem.* **2012**, *16*, 2127–2133.
- (38) Goto, T. E.; Lopez, R. F.; Oliveira, O. N., Jr.; Caseli, L. Enzyme Activity of Catalase Immobilized in Langmuir–Blodgett Films of Phospholipids. *Langmuir* **2010**, *26*, 11135–11139.
- (39) Caseli, L.; Crespilho, F. N.; Nobre, T. M.; Zaniquelli, M. E. D.; Zucolotto, V.; Oliveira, O. N., Jr. Using phospholipid Langmuir and Langmuir–Blodgett Films as Matrix for Urease Immobilization. *J. Colloid Interface Sci.* **2008**, *319*, 100–108.
- (40) Godoy, S.; Chauvet, J. P.; Boullanger, P.; Blum, L. J.; Girard-Egrot, A. P. New Functional Proteo-Glycolipidic Molecular Assembly for Biocatalysis Analysis of an Immobilized Enzyme in a Biomimetic Nanostructure. *Langmuir* **2003**, *19*, 5448–5456.
- (41) Crespilho, F. N.; Zucolotto, V.; Oliveira, O. N., Jr.; Nart, F. C. Electrochemistry of Layer-by-Layer Films: A Review. *Int. J. Electrochem. Sci.* **2006**, *1*, 194–214.
- (42) Cao, T. B.; Chen, J. Y.; Yang, C. H.; Cao, W. X. Fabrication of a Stable Layer-by-Layer Thin Film Based on Diazo-resin and Phenolic Hydroxy-Containing Polymers via H-bonding. *Macromol. Rapid Commun.* **2001**, *22*, 181–184.
- (43) Yang, W. J.; Trau, D.; Renneberg, R.; Yu, N. T.; Caruso, F. Layer-by-Layer Construction of Novel Biofunctional Fluorescent Micro-particles for Immunoassay Applications. *J. Colloid Interface Sci.* **2001**, *234*, 356–362.
- (44) Caseli, L.; Tiburcio, V. L. B.; Vargas, F. F. R.; Marangoni, S.; Siqueira, J. R., Jr. Enhanced Architecture of Lipid-Carbon Nanotubes as Langmuir–Blodgett Films To Investigate the Enzyme Activity of Phospholipases from Snake Venom. *J. Phys. Chem. B* **2012**, *116*, 13424–13429.
- (45) Ma, J. B.; Cai, P.; Qi, W.; Kong, D. S.; Wang, H. The Layer-by-Layer Assembly of Polyelectrolyte Functionalized Graphene Sheets: A Potential Tool for Biosensing. *Colloids Surf., A* **2013**, *426*, 6–11.
- (46) Vieira, N. C. S.; Figueiredo, A.; Faceto, A. D.; de Queiroz, A. A. A.; Zucolotto, V.; Guimaraes, F. E. G. Dendrimers/TiO<sub>2</sub> Nanoparticles Layer-by-Layer Films as Extended Gate FET for pH Detection. *Sens. Actuators, B* **2012**, *169*, 397–400.
- (47) Crespilho, F. N.; Ghica, M. E.; Florescu, M.; Nart, F. C.; Oliveira, O. N., Jr.; Brett, C. M. A. A Strategy for Enzyme Immobilization on Layer-by-Layer Dendrimer-Gold Nanoparticle Electrochemical Membrane Incorporating Redox Mediator. *Electrochem. Commun.* **2006**, *8*, 1665–1670.
- (48) Claussen, J. C.; Kumar, A.; Jaroch, D. B.; Khawaja, M. H.; Hibbard, A. B.; Porterfield, D. M.; Fisher, T. S. Nanostructuring Platinum Nanoparticles on Multilayered Graphene Petal Nanosheets for Electrochemical Biosensing. *Adv. Funct. Mater.* **2012**, *22*, 3399–3405.
- (49) Arya, S. K.; Solanki, P. R.; Datta, M.; Malhotra, B. D. Recent Advances in Self-Assembled Monolayers Based Biomolecular Electronic Devices. *Biosens. Bioelectron.* **2009**, *24*, 2810–2817.
- (50) Maoz, R.; Netzer, L.; Gun, J.; Sagiv, J. Self-Assembling Monolayers in the Construction of Planned Supramolecular Sutures and as Modifiers of Surface-Properties. *J. Chim. Phys. Phys.-Chim. Biol.* **1988**, *85*, 1059–1065.
- (51) Gooding, J. J.; Darwish, N. The Rise of Self-Assembled Monolayers for Fabricating Electrochemical Biosensors—An Interfacial Perspective. *Chem. Rev.* **2012**, *12*, 92–105.
- (52) Booth, M. A.; Vogel, R.; Curran, J. M.; Harbison, S.; Trivas-Sejdic, J. Detection of Target–Probe Oligonucleotide Hybridization Using

Synthetic Nanopore Resistive Pulse Sensing. *Biosens. Bioelectron.* **2013**, *45*, 136–140.

(53) Bard, A. J.; Denault, G.; Friesner, R. A.; Dornblaser, B. C.; Tuckerman, L. S. Scanning Electrochemical Microscopy—Theory and Application of the Transient (Chronoamperometric) SECM Response. *Anal. Chem.* **1991**, *63*, 1282–1288.

(54) Ebejer, N.; Guell, A. G.; Lai, S. C. S.; McKelvey, K.; Snowden, M. E.; Unwin, P. R. Scanning Electrochemical Cell Microscopy: A Versatile Technique for Nanoscale Electrochemistry and Functional Imaging. *Annu. Rev. Anal. Chem.* **2013**, *6*, 329–351.

(55) Kleijn, S. E. F.; Lai, S. C. S.; Miller, T. S.; Yanson, A. I.; Koper, M. T. M.; Unwin, P. R. Landing and Catalytic Characterization of Individual Nanoparticles on Electrode Surfaces. *J. Am. Chem. Soc.* **2012**, *134*, 18558–18561.

(56) Yamashita, K.; Takagi, M.; Uchida, K.; Kondo, H.; Takenaka, S. Visualization of DNA Microarrays by Scanning Electrochemical Microscopy (SECM). *Analyst* **2001**, *126*, 1210–1211.

(57) Novoselov, K. S.; Geim, A. K.; Morozov, S. V.; Jiang, D.; Zhang, Y.; Dubonos, S. V.; Grigorieva, I. V.; Firsov, A. A. Electric Field Effect in Atomically Thin Carbon Films. *Science* **2004**, *306*, 666–669.

(58) Geim, A. K.; Novoselov, K. S. The Rise of Graphene. *Nat. Mater.* **2007**, *6*, 183–191.

(59) Banerjee, S.; Shim, J.; Rivera, J.; Jin, X. Z.; Estrada, D.; Solovyeva, V.; You, X.; Pak, J.; Pop, E.; Aluru, N.; Bashir, R. Electrochemistry at the Edge of a Single Graphene Layer in a Nanopore. *ACS Nano* **2013**, *7*, 834–843.

(60) Zheng, N.; Fan, J.; Stucky, G. D. One-Step One-Phase Synthesis of Monodisperse Noble-Metallic Nanoparticles and Their Colloidal Crystals. *J. Am. Chem. Soc.* **2006**, *128*, 6550–6551.

(61) Correia, A. N.; Mascaró, L. H.; Machado, S. A. S.; Mazo, L. H.; Avaca, L. A. Ultramicroelectrodes 0.1. Theoretical Revision and Outlook. *Quim. Nova* **1995**, *18*, 475–480.

(62) Zoski, C. G. Ultramicroelectrodes: Design, Fabrication, and Characterization. *Electroanalysis* **2002**, *14*, 1041–1051.

(63) Sone, J.; Fujita, J.; Ochiai, Y.; Manako, S.; Matsui, S.; Nomura, E.; Baba, T.; Kawaura, H.; Sakamoto, T.; Chen, C. D.; Nakamura, Y.; Tsai, J. S. Nanofabrication toward sub-10 nm and Its Application to Novel Nanodevices. *Nanotechnology* **1999**, *10*, 135–141.

(64) Dickinson, E. J. F.; Compton, R. G. Diffuse Double Layer at Nanoelectrodes. *J. Phys. Chem. C* **2009**, *113*, 17585–17589.

(65) Murray, R. W. Nanoelectrochemistry: Metal Nanoparticles, Nanoelectrodes, and Nanopores. *Chem. Rev.* **2008**, *108*, 2688–2720.

(66) Sun, P.; Mirkin, M. V. Kinetics of Electron-Transfer Reactions at Nanoelectrodes. *Anal. Chem.* **2006**, *78*, 6526–6534.

(67) Goncalves, W. D.; Lanfredi, A. J. C.; Crespilho, F. N. Development of Numerical Methods for Signal Smoothing and Noise Modeling in Single Wire-Based Electrochemical Biosensors. *J. Phys. Chem. C* **2011**, *115*, 16172–16179.

(68) Besteman, K.; Lee, J. O.; Wiertz, F. G. M.; Heering, H. A.; Dekker, C. Enzyme-Coated Carbon Nanotubes as Single-Molecule Biosensors. *Nano Lett.* **2003**, *3*, 727–730.

(69) Crespilho, F. N.; Lanfredi, A. J. C.; Leite, E. R.; Chiquito, A. J. Development of Individual Semiconductor Nanowire for Bioelectrochemical Device at Low Overpotential Conditions. *Electrochem. Commun.* **2009**, *11*, 1744–1747.

(70) Siqueira, J. R., Jr.; Caseli, L.; Crespilho, F. N.; Zucolotto, V.; Oliveira, O. N., Jr. Immobilization of Biomolecules on Nanostructured Films for Biosensing. *Biosens. Bioelectron.* **2010**, *25*, 1254–1263.

(71) Schöning, M. J.; Poghossian, A. Bio FEDs (Field-Effect Devices): State-of-the-Art and New Directions. *Electroanalysis* **2006**, *18*, 1893–1900.

(72) Patolsky, F.; Timko, B. P.; Zheng, G. F.; Lieber, C. M. Nanowire-Based Nanoelectronic Devices in the Life Sciences. *MRS Bull.* **2007**, *32*, 142–149.

(73) Cui, T. H.; Hua, F.; Lvov, Y. FET Fabricated by Layer-by-Layer Nanoassembly. *IEEE Trans. Electron Devices* **2004**, *51*, 503–506.

(74) Xu, J. J.; Zhao, W.; Luo, X. L.; Chen, H. Y. A Sensitive Biosensor for Lactate Based on Layer-by-Layer Assembling MnO<sub>2</sub> Nanoparticles

and Lactate Oxidase on Ion-Sensitive Field-Effect Transistors. *Chem. Commun.* **2005**, *14*, 792–794.

(75) Javey, A.; Nam, S.; Friedman, R. S.; Yan, H.; Lieber, C. M. Layer-by-Layer Assembly of Nanowires for Three-Dimensional, Multifunctional Electronics. *Nano Lett.* **2007**, *7*, 773–777.

(76) Poghossian, A.; Ingebrandt, S.; Abouzar, M. H.; Schöning, M. J. Label-Free Detection of Charged Macromolecules by Using a Field-Effect-Based Sensor Platform: Experiments and Possible Mechanisms of Signal Generation. *Appl. Phys. A: Mater. Sci. Process.* **2007**, *87*, 517–524.

(77) Gauglitz, G. Direct Optical Sensors: Principles and Selected Applications. *Anal. Bioanal. Chem.* **2005**, *381*, 141–155.

(78) Schmidt, T. F.; Caseli, L.; dos Santos, D. S., Jr.; Oliveira, O. N., Jr. Enzyme Activity of Horseradish Peroxidase Immobilized in Chitosan Matrices in Alternated Layers. *Mater. Sci. Eng., C* **2009**, *29*, 1889–1892.

(79) Schmidt, T. F.; Caseli, L.; Viitala, T.; Oliveira, O. N., Jr. Enhanced Activity of Horseradish Peroxidase in Langmuir–Blodgett Films of Phospholipids. *Biochim. Biophys. Acta, Biomembr.* **2008**, *1778*, 2291–2297.

(80) Willner, I.; Willner, B. Biomolecule-Based Nanomaterials and Nanostructures. *Nano Lett.* **2010**, *10*, 3805–3815.

(81) Wegner, K. D.; Lanh, P. T.; Jennings, T.; Oh, E.; Jain, V.; Fairclough, S. M.; Smith, J. M.; Giovanelli, E.; Lequeux, N.; Pons, T.; Hildebrandt, N. Influence of Luminescence Quantum Yield, Surface Coating, and Functionalization of Quantum Dots on the Sensitivity of Time-Resolved FRET Bioassays. *ACS Appl. Mater. Interfaces* **2013**, *5*, 2881–2892.

(82) Jiang, C. F.; Zhao, T. T.; Li, S.; Gao, N. Y.; Xu, Q. H. Highly Sensitive Two-Photon Sensing of Thrombin in Serum Using Aptamers and Silver Nanoparticles. *ACS Appl. Mater. Interfaces* **2013**, *5*, 10853–10857.

(83) Bhuvana, T.; Kulkarni, G. U. A SERS-Activated Nanocrystalline Pd Substrate and Its Nanopatterning Leading to Biochip Fabrication. *Small* **2008**, *4*, 670–676.

(84) Wang, L. Y.; Sun, Y.; Wang, J.; Zhu, X. N.; Jia, F.; Cao, Y. B.; Wang, X. H.; Zhang, H. Q.; Song, D. Q. Sensitivity Enhancement of SPR Biosensor with Silver Mirror Reaction on the Ag/Au Film. *Talanta* **2009**, *78*, 265–269.

(85) Kara, M.; Uzun, L.; Kolayli, S.; Denizli, A. Combining Molecular Imprinted Nanoparticles with Surface Plasmon Resonance Nanosensor for Chloramphenicol Detection in Honey. *J. Appl. Polym. Sci.* **2013**, *129*, 2273–2279.

(86) Silva, A. C. A.; de Deus, S. L. V.; Silva, M. J. B.; Dantas, N. O. Highly Stable luminescence of CdSe Magic-Sized Quantum Dots in HeLa Cells. *Sens. Actuators, B* **2014**, *191*, 108–114.

(87) Peng, C. W.; Li, Y. Application of Quantum Dots-Based Biotechnology in Cancer Diagnosis: Current Status and Future Perspectives. *J. Nanomater.* **2010**, 1–11.

(88) Clift, M. J. D.; Stone, V. Quantum Dots: An Insight and Perspective of Their Biological Interaction and How This Relates to Their Relevance for Clinical Use. *Theranostics* **2012**, *2*, 668–680.

(89) Smith, A. M.; Dave, S.; Nie, S. M.; True, L.; Gao, X. H. Multicolor Quantum Dots for Molecular Diagnostics of Cancer. *Expert Rev. Mol. Diagn.* **2006**, *6*, 231–244.

(90) Jain, K. K. Applications of Nanobiotechnology in Clinical Diagnostics. *Clin. Chem.* **2007**, *53*, 2002–2009.

(91) Azzazy, H. M. E.; Mansour, M. M. H.; Kazmierczak, S. C. From Diagnostics to Therapy: Prospects of Quantum Dots. *Clin. Biochem.* **2007**, *40*, 917–927.

(92) Azzazy, H. M. E.; Mansour, M. M. H.; Kazmierczak, S. C. Nanodiagnostics: A New Frontier for Clinical Laboratory Medicine. *Clin. Chem.* **2006**, *52*, 1238–1246.

(93) Wang, H. Z.; Wang, H. Y.; Liang, R. Q.; Ruan, K. C. Detection of Tumor Marker CA125 in Ovarian Carcinoma Using Quantum Dots. *Acta Biochim. Biophys. Sin.* **2004**, *36*, 681–686.

(94) Nathwani, B. B.; Jaffari, M.; Juriani, A. R.; Mathur, A. B.; Meissner, K. E. Fabrication and Characterization of Silk-Fibroin-Coated Quantum Dots. *IEEE Trans. Nanobiosci.* **2009**, *8*, 72–77.

(95) Wu, X. Y.; Liu, H. J.; Liu, J. Q.; Haley, K. N.; Treadway, J. A.; Larson, J. P.; Ge, N. F.; Peale, F.; Bruchez, M. P. Immunofluorescent

Labeling of Cancer Marker Her2 and Other Cellular Targets with Semiconductor Quantum Dots. *Nat. Biotechnol.* **2003**, *21*, 41–46.

(96) Yezhelyev, M. V.; Al-Hajj, A.; Morris, C.; Marcus, A. I.; Liu, T.; Lewis, M.; Cohen, C.; Zrazhevskiy, P.; Simons, J. W.; Rogatko, A.; Nie, S.; Gao, X.; O'Regan, R. M. In Situ Molecular Profiling of Breast Cancer Biomarkers with Multicolor Quantum Dots. *Adv. Mater.* **2007**, *19*, 3146–3151.

(97) Smith, A. M.; Duan, H. W.; Mohs, A. M.; Nie, S. M. Bioconjugated Quantum Dots for in Vivo Molecular and Cellular Imaging. *Adv. Drug Delivery Rev.* **2008**, *60*, 1226–1240.

(98) Gao, X.; Chung, L. W.; Nie, S. Quantum Dots for in Vivo Molecular and Cellular Imaging. *Methods Mol. Biol.* **2007**, *374*, 135–145.

(99) Barua, S.; Rege, K. Cancer-Cell-Phenotype-Dependent Differential Intracellular Trafficking of Unconjugated Quantum Dots. *Small* **2009**, *5*, 370–376.

(100) Yang, L.; Mao, H.; Wang, Y. A.; Cao, Z.; Peng, X.; Wang, X.; Duan, H.; Ni, C.; Yuan, Q.; Adams, G.; Smith, M. Q.; Wood, W. C.; Gao, X.; Nie, S. Single Chain Epidermal Growth Factor Receptor Antibody Conjugated Nanoparticles for in Vivo Tumor Targeting and Imaging. *Small* **2009**, *5*, 235–243.

(101) Yong, K. T. Mn-Doped Near-Infrared Quantum Dots as Multimodal Targeted Probes for Pancreatic Cancer Imaging. *Nanotechnology* **2009**, *20*, 1–10.

(102) Kim, S. N.; Rusling, J. F.; Papadimitrakopoulos, F. Carbon Nanotubes for Electronic and Electrochemical Detection of Biomolecules. *Adv. Mater.* **2007**, *19*, 3214–3228.

(103) Balasubramanian, K.; Burghard, M. Electrochemically Functionalized Carbon Nanotubes for Device Applications. *J. Mater. Chem.* **2008**, *18*, 3071–3083.

(104) Balasubramanian, K.; Burghard, M.; Kern, K. Effect of the Electronic Structure of Carbon Nanotubes on the Selectivity of Electrochemical Functionalization. *Phys. Chem. Chem. Phys.* **2008**, *10*, 2256–2262.

(105) Balasubramanian, K.; Lee, E. J. H.; Weitz, R. T.; Burghard, M.; Kern, K. Carbon Nanotube Transistors—Chemical Functionalization and Device Characterization. *Phys. Status Solidi A* **2008**, *205*, 633–646.

(106) Allen, B. L.; Kichambare, P. D.; Star, A. Carbon Nanotube Field-Effect-Transistor-Based Biosensors. *Adv. Mater.* **2007**, *19*, 1439–1451.

(107) Balasubramanian, K.; Burghard, M. Biosensors Based on Carbon Nanotubes. *Anal. Bioanal. Chem.* **2006**, *385*, 452–468.

(108) Heller, I.; Kong, J.; Heering, H. A.; Williams, K. A.; Lemay, S. G.; Dekker, C. Individual Single-Walled Carbon Nanotubes as Nanoelectrodes for Electrochemistry. *Nano Lett.* **2005**, *5*, 137–142.

(109) Dudin, P. V.; Snowden, M. E.; Macpherson, J. V.; Unwin, P. R. Electrochemistry at Nanoscale Electrodes: Individual Single-Walled Carbon Nanotubes (SWNTs) and SWNT-Templated Metal Nanowires. *ACS Nano* **2011**, *5*, 10017–10025.

(110) Siqueira, J. R., Jr.; Bäcker, M.; Poghosian, A.; Zucolotto, V.; Oliveira, O. N., Jr.; Schöning, M. J. Associating Biosensing Properties with the Morphological Structure of Multilayers Containing Carbon Nanotubes on Field-Effect Devices. *Phys. Status Solidi A* **2010**, *20*, 781–786.

(111) Siqueira, J. R., Jr.; Abouzar, M. H.; Poghosian, A.; Zucolotto, V.; Oliveira, O. N., Jr.; Schöning, M. J. Penicillin Biosensor Based on a Capacitive Field-Effect Structure Functionalized with a Dendrimer/Carbon Nanotube Multilayer. *Biosens. Bioelectron.* **2009**, *25*, 497–501.

(112) Castro Neto, A. H.; Guinea, F.; Peres, N. M. R.; Novoselov, K. S.; Geim, A. K. The Electronic Properties of Graphene. *Rev. Mod. Phys.* **2009**, *81*, 109–162.

(113) Ping, J. F.; Wang, Y. X.; Fan, K.; Wu, J.; Ying, Y. B. Direct Electrochemical Reduction of Graphene Oxide on Ionic Liquid Doped Screen-Printed Electrode and Its Electrochemical Biosensing Application. *Biosens. Bioelectron.* **2011**, *28*, 204–209.

(114) Suk, J. W.; Kitt, A.; Magnuson, C. W.; Hao, Y. F.; Ahmed, S.; An, J. H.; Swan, A. K.; Goldberg, B. B.; Ruoff, R. S. Transfer of CVD-Grown Monolayer Graphene onto Arbitrary Substrates. *ACS Nano* **2011**, *5*, 6916–6924.

(115) Hummers, W. S.; Offeman, R. E. Preparation of Graphitic Oxide. *J. Am. Chem. Soc.* **1958**, *80*, 1339–1339.

(116) Higginbotham, A. L.; Kosynkin, D. V.; Sinitzki, A.; Sun, Z. Z.; Tour, J. M. Lower-Defect Graphene Oxide Nanoribbons from Multiwalled Carbon Nanotubes. *ACS Nano* **2010**, *4*, 2059–2069.

(117) Chua, C. K.; Pumera, M. Chemical Reduction of Graphene Oxide: A Synthetic Chemistry Viewpoint. *Chem. Soc. Rev.* **2014**, *43*, 291–312.

(118) Hirsch, A.; Englert, J. M.; Hauke, F. Wet Chemical Functionalization of Graphene. *Acc. Chem. Res.* **2013**, *46*, 87–96.

(119) Zhang, T.; Cheng, Z. G.; Wang, Y. B.; Li, Z. J.; Wang, C. X.; Li, Y. B.; Fang, Y. Self-Assembled 1-Octadecanethiol Monolayers on Graphene for Mercury Detection. *Nano Lett.* **2010**, *10*, 4738–4741.

(120) Bao, H. Q.; Pan, Y. Z.; Ping, Y.; Sahoo, N. G.; Wu, T. F.; Li, L.; Li, J.; Gan, L. H. Chitosan-Functionalized Graphene Oxide as a Nanocarrier for Drug and Gene Delivery. *Small* **2011**, *7*, 1569–1578.

(121) Bo, Y.; Yang, H. Y.; Hu, Y.; Yao, T. M.; Huang, S. S. A Novel Electrochemical DNA Biosensor Based on Graphene and Polyaniline Nanowires. *Electrochim. Acta* **2011**, *56*, 2676–2681.

(122) Akhavan, O.; Ghaderi, E.; Rahighi, R. Toward Single-DNA Electrochemical Biosensing by Graphene Nanowalls. *ACS Nano* **2012**, *6*, 2904–2916.

(123) Ambrosi, A.; Pumera, M. Stacked Graphene Nanofibers for Electrochemical Oxidation of DNA Bases. *Phys. Chem. Chem. Phys.* **2010**, *12*, 8944–8948.

(124) Wang, Y.; Shao, Y. Y.; Matson, D. W.; Li, J. H.; Lin, Y. H. Nitrogen-Doped Graphene and Its Application in Electrochemical Biosensing. *ACS Nano* **2010**, *4*, 1790–1798.

(125) Nandini, S.; Nalini, S.; Manjunatha, R.; Shanmugam, S.; Melo, J. S.; Suresh, G. S. Electrochemical Biosensor for the Selective Determination of Hydrogen Peroxide Based on the Co-deposition of Palladium, Horseradish Peroxidase on Functionalized-Graphene Modified Graphite Electrode as Composite. *J. Electroanal. Chem.* **2013**, *689*, 233–242.

(126) Zhang, N.; Lv, X. Y.; Ma, W. G.; Hu, Y. W.; Li, F. H.; Han, D. X.; Niu, L. Direct Electron Transfer of Cytochrome C at Mono-Dispersed and Negatively Charged Perylene-Graphene Matrix. *Talanta* **2013**, *107*, 195–202.

(127) Oliveira, T. M. B. F.; Barroso, M. F.; Morais, S.; Araujo, M.; Freire, C.; de Lima-Neto, P.; Correia, A. N.; Oliveira, M. B. P. P.; Delerue-Matos, C. Laccase-Prussian Blue Film-Graphene Doped Carbon Paste Modified Electrode for Carbamate Pesticides Quantification. *Biosens. Bioelectron.* **2013**, *47*, 292–299.

(128) Feng, Q. L.; Du, Y. L.; Zhang, C.; Zheng, Z. X.; Hu, F. D.; Wang, Z. H.; Wang, C. M. Synthesis of the Multi-Walled Carbon Nanotubes-COOH/Graphene/Gold Nanoparticles Nanocomposite for Simple Determination of Bilirubin in Human Blood Serum. *Sens. Actuators, B* **2013**, *185*, 337–344.

(129) Xing, Z. C.; Tian, J. Q.; Asiri, A. M.; Qusti, A. H.; Al-Youbi, A. O.; Sun, X. P. Two-Dimensional Hybrid Mesoporous Fe<sub>2</sub>O<sub>3</sub>-Graphene Nanostructures: A Highly Active and Reusable Peroxidase Mimetic toward Rapid, Highly Sensitive Optical Detection of Glucose. *Biosens. Bioelectron.* **2014**, *52*, 452–457.

(130) Balasubramanian, K.; Kern, K. Label-Free Electrical Bio-detection Using Carbon Nanostructures. *Adv. Mater.* **2014**, *26*, 1154–1175.

(131) Traversi, F.; Raillon, C.; Benameur, S. M.; Liu, K.; Khlybov, S.; Tosun, M.; Krasnozhan, D.; Kis, A.; Radenovic, A. Detecting the Translocation of DNA through a Nanopore Using Graphene Nanoribbons. *Nat. Nanotechnol.* **2013**, *8*, 939–945.

(132) Min, S. K.; Kim, W. Y.; Cho, Y.; Kim, K. S. Fast DNA Sequencing with a Graphene-Based Nanochannel Device. *Nat. Nanotechnol.* **2011**, *6*, 162–165.

(133) Li, Y. Y.; Ma, J. P.; Zhu, H. Y.; Gao, X. L.; Dong, H. Q.; Shi, D. L. Green Synthetic Multifunctional Hybrid Micelles with Shell Embedded Magnetic Nanoparticles for Theranostic Applications. *ACS Appl. Mater. Interfaces* **2013**, *5*, 7227–7235.

(134) Peng, S.; Zheng, Q.; Zhang, X.; Dai, L. H.; Zhu, J. X.; Pi, Y. B.; Hu, X. G.; Cheng, W. Q.; Zhou, C. Y.; Sha, Y. L.; Ao, Y. F. Detection of ADAMTS-4 Activity Using a Fluorogenic Peptide-Conjugated Au

Nanoparticle Probe in Human Knee Synovial Fluid. *ACS Appl. Mater. Interfaces* **2013**, *5*, 6089–6096.

(135) Hirsch, R.; Katz, E.; Willner, I. Magneto-Switchable Bioelectrocatalysis. *J. Am. Chem. Soc.* **2000**, *122*, 12053–12054.

(136) Katz, E.; Sheeney-Haj-Ichia, L.; Buckmann, A. F.; Willner, I. Dual Biosensing by Magneto-Controlled Bioelectrocatalysis. *Angew. Chem., Int. Ed.* **2002**, *41*, 1343–1346.

(137) Katz, E.; Sheeney-Haj-Ichia, L.; Willner, I. Magneto-Switchable Electrochemical and Bioelectrocatalytic Transformations. *Chem.—Eur. J.* **2002**, *8*, 4138–4148.

(138) Katz, E.; Lioubashevski, O.; Willner, I. Magnetic Field Effects on Bioelectrocatalytic Reactions of Surface-Confined Enzyme Systems: Enhanced Performance of Biofuel Cells. *J. Am. Chem. Soc.* **2005**, *127*, 3979–3988.

(139) Liang, C.; Jing, L.; Shi, X. H.; Zhang, Y. X.; Xian, Y. Z. Magnetically Controlled Bioelectrocatalytic System Based on Ferrocene-Tagged Magnetic Nanoparticles by Thiol-Ene Reaction. *Electrochim. Acta* **2012**, *69*, 167–173.

(140) Melo, A. F. A. A.; Luz, R. A. S.; Iost, R. M.; Nantes, I. L.; Crespihlo, F. N. Highly Stable Magnetite Modified with Chitosan, Ferrocene and Enzyme for Application in Magneto-Switchable Bioelectrocatalysis. *J. Brazil. Chem. Soc.* **2013**, *24*, 285–294.

(141) Melo, A. F. A. A.; Carvalho, V. A. N.; Pagnoncelli, K. C.; Crespihlo, F. N. Single Microparticle Applied in Magnetic-Switchable Electrochemistry. *Electrochem. Commun.* **2013**, *30*, 79–82.

(142) Lima, K. M. G.; Araújo, R. F., Jr.; Araujo, A. A.; Oliveira, A. L. C. S. L.; Gasparotto, L. H. S. Environmentally Compatible Bioconjugated Gold Nanoparticles as Efficient Contrast Agents for Colorectal Cancer Cell Imaging. *Sens. Actuators, B* **2014**, *196*, 306–313.

(143) Marangoni, V. S.; Paino, I. M.; Zucolotto, V. Synthesis and Characterization of Jacalin-Gold Nanoparticles Conjugates as Specific Markers for Cancer Cells. *Colloids Surf., B* **2013**, *112*, 380–386.

(144) Paul, S.; Planque, S. A.; Nishiyama, Y.; Hanson, C. V.; Massey, R. J. Nature and Nurture of Catalytic Antibodies. *Adv. Exp. Med. Biol.* **2012**, *750*, 56–75.

(145) Dickerson, T. J.; Yamamoto, N.; Janda, K. D. Antibody-Catalyzed Oxidative Degradation of Nicotine Using Riboflavin. *Bioorgan. Med. Chem.* **2004**, *12*, 4981–4987.

(146) Shabat, D.; Grynszpan, F.; Saphier, S.; Turniansky, A.; Avnir, D.; Keinan, E. An Efficient Sol-Gel Reactor for Antibody-Catalyzed Transformations. *Chem. Mater.* **1997**, *9*, 2258–2260.

(147) Mu, Y.; Song, D. Q.; Li, Y.; Zhang, H. Q.; Li, W.; Luo, G. M.; Jin, Q. H. Selection of Phage Antibodies with GPX Activity by Combination of Phage Displayed Antibody Library with Chemical Modification and Their Characterization Using a Surface Plasmon Resonance Biosensor. *Talanta* **2005**, *66*, 181–187.

(148) Blackburn, G. F.; Talley, D. B.; Booth, P. M.; Durfor, C. N.; Martin, M. T.; Napper, A. D.; Rees, A. R. Potentiometric Biosensor Employing Catalytic Antibodies as the Molecular Recognition Element. *Anal. Chem.* **1990**, *62*, 2211–2216.

(149) Yang, G. S.; Ying, L.; Ou, Z. M.; Yao, S. J. Resolution of Ibuprofen Ester by Catalytic Antibodies in Water-Miscible Organic Solvents. *Chin. J. Chem. Eng.* **2009**, *17*, 506–512.

(150) Gill, I.; Ballesteros, A. Bioencapsulation within Synthetic Polymers (Part 1): Sol-Gel Encapsulated Biologicals. *Trends Biotechnol.* **2000**, *18*, 282–296.

(151) Iost, R. M.; da Silva, W. C.; Madurro, J. M.; Madurro, A. G.; Ferreira, L. F.; Crespihlo, F. N. Recent Advances in Nano-Based Electrochemical Biosensors: Application in Diagnosis and Monitoring of Diseases. *Front. Biosci., Elite Ed.* **2011**, *3*, 663–89.

(152) Zhai, J.; Cui, H.; Yang, R. DNA Based Biosensors. *Biotechnol. Adv.* **1997**, *15*, 43–58.

(153) Balasubramanian, K. Label-Free Indicator-Free Nucleic Acid Biosensors Using Carbon Nanotubes. *Eng. Life Sci.* **2012**, *12*, 121–130.

(154) Millan, K. M.; Mikkelsen, S. R. Sequence-Selective Biosensor for DNA-Based on Electroactive Hybridization Indicators. *Anal. Chem.* **1993**, *65*, 2317–2323.

(155) Steinem, C.; Janshoff, A.; Lin, V. S. Y.; Volcker, N. H.; Ghadiri, M. R. DNA Hybridization-Enhanced Porous Silicon Corrosion:

Mechanistic Investigations and Prospect for Optical Interferometric Biosensing. *Tetrahedron* **2004**, *60*, 11259–11267.

(156) Lucarelli, F.; Tombelli, S.; Minunni, M.; Marrazza, G.; Mascini, M. Electrochemical and Piezoelectric DNA Biosensors for Hybridisation Detection. *Anal. Chim. Acta* **2008**, *609*, 139–159.

(157) Lin, C. T.; Loan, P. T. K.; Chen, T. Y.; Liu, K. K.; Chen, C. H.; Wei, K. H.; Li, L. J. Label-Free Electrical Detection of DNA Hybridization on Graphene Using Hall Effect Measurements: Revisiting the Sensing Mechanism. *Adv. Funct. Mater.* **2013**, *23*, 2301–2307.

(158) Zeng, L. X.; Zhang, A. Z.; Zhu, X. H.; Zhang, C. Y.; Liang, Y.; Nan, J. M. Electrochemical Determination of Nonylphenol Using Differential Pulse Voltammetry Based on a Graphene-DNA-Modified Glassy Carbon Electrode. *J. Electroanal. Chem.* **2013**, *703*, 153–157.

(159) Kizek, R.; Havran, L.; Fojta, M.; Palecek, E. Determination of Nanogram Quantities of Osmium-Labeled Single Stranded DNA by Differential Pulse Stripping Voltammetry. *Bioelectrochemistry* **2002**, *55*, 119–121.

(160) Caruso, F.; Rodda, E.; Furlong, D. F.; Niikura, K.; Okahata, Y. Quartz Crystal Microbalance Study of DNA Immobilization and Hybridization for Nucleic Acid Sensor Development. *Anal. Chem.* **1997**, *69*, 2043–2049.

(161) Guo, Z. J.; Sadler, P. J.; Tsang, S. C. Immobilization and Visualization of DNA and Proteins on Carbon Nanotubes. *Adv. Mater.* **1998**, *10*, 701–703.

(162) Cai, H.; Cao, X. N.; Jiang, Y.; He, P. G.; Fang, Y. Z. Carbon Nanotube-Enhanced Electrochemical DNA Biosensor for DNA Hybridization Detection. *Anal. Bioanal. Chem.* **2003**, *375*, 287–293.

(163) Zhao, H. Q.; Lin, L.; Li, J. R.; Tang, J. A.; Duan, M. X.; Jiang, L. DNA Biosensor with High Sensitivity Amplified by Gold Nanoparticles. *J. Nanopart. Res.* **2001**, *3*, 321–323.

(164) Zhang, Y. Z.; Zhang, K. Y.; Ma, H. Y. Electrochemical DNA Biosensor Based on Silver Nanoparticles/Poly(3-(3-pyridyl) Acrylic Acid)/Carbon Nanotubes Modified Electrode. *Anal. Biochem.* **2009**, *387*, 13–19.

(165) Ma, L. P.; Yuan, R.; Chai, Y. Q.; Chen, S. H. Amperometric Hydrogen Peroxide Biosensor Based on the Immobilization of HRP on DNA-Silver Nanohybrids and PDDA-Protected Gold Nanoparticles. *J. Mol. Catal. B: Enzym.* **2009**, *56*, 215–220.

(166) Ma, H. Y.; Zhang, L. P.; Pan, Y.; Zhang, K. Y.; Zhang, Y. Z. A Novel Electrochemical DNA Biosensor Fabricated with Layer-by-Layer Covalent Attachment of Multiwalled Carbon Nanotubes and Gold Nanoparticles. *Electroanalysis* **2008**, *20*, 1220–1226.

(167) Lin, L.; Liu, Y.; Tang, L. H.; Li, J. H. Electrochemical DNA Sensor by the Assembly of Graphene and DNA-Conjugated Gold Nanoparticles with Silver Enhancement Strategy. *Analyst* **2011**, *136*, 4732–4737.

(168) Wang, J. X.; Yi, X. Y.; Tang, H. L.; Han, H. X.; Wu, M. H.; Zhou, F. M. Direct Quantification of MicroRNA at Low Picomolar Level in Sera of Glioma Patients Using a Competitive Hybridization Followed by Amplified Voltammetric Detection. *Anal. Chem.* **2012**, *84*, 6400–6406.

(169) Dong, X. C.; Shi, Y. M.; Huang, W.; Chen, P.; Li, L. J. Electrical Detection of DNA Hybridization with Single-Base Specificity Using Transistors Based on CVD-Grown Graphene Sheets. *Adv. Mater.* **2010**, *22*, 1649–1653.

(170) Niu, S. Y.; Han, B.; Cao, W.; Zhang, S. S. Sensitive DNA Biosensor Improved by Luteolin Copper(II) as Indicator Based on Silver Nanoparticles and Carbon Nanotubes Modified Electrode. *Anal. Chim. Acta* **2009**, *651*, 42–47.

(171) Ye, J. S.; Wen, Y.; Zhang, W. D.; Gan, L. M.; Xu, G. Q.; Sheu, F. S. Nonenzymatic Glucose Detection Using Multi-Walled Carbon Nanotube Electrodes. *Electrochem. Commun.* **2004**, *6*, 66–70.

(172) Clark, L. C.; Lyons, C. Electrode Systems for Continuous Monitoring in Cardiovascular Surgery. *Ann. N.Y. Acad. Sci.* **1962**, *102*, 29–45.

(173) Tang, D. Y.; Xia, B. Y. Electrochemical Immunosensor and Biochemical Analysis for Carcinoembryonic Antigen in Clinical Diagnosis. *Microchim. Acta* **2008**, *163*, 41–48.

- (174) Fu, X. H. Magnetic-Controlled Non-competitive Enzyme-Linked Voltammetric Immunoassay for Carcinoembryonic Antigen. *Biochem. Eng. J.* **2008**, *39*, 267–275.
- (175) Ariga, K.; Ji, Q. M.; Mori, T.; Naito, M.; Yamauchi, Y.; Abe, H.; Hill, J. P. Enzyme Nanoarchitectonics: Organization and Device Application. *Chem. Soc. Rev.* **2013**, *42*, 6322–6345.
- (176) Vidal, J. C.; Garcia, E.; Castillo, J. R. In Situ Preparation of a Cholesterol Biosensor: Entrapment of Cholesterol Oxidase in an Overoxidized Polypyrrole Film Electrodeposited in a Flow System – Determination of Total Cholesterol in Serum. *Anal. Chim. Acta* **1999**, *385*, 213–222.
- (177) Singh, S.; Chaubey, A.; Malhotra, B. D. Amperometric Cholesterol Biosensor Based on Immobilized Cholesterol Esterase and Cholesterol Oxidase on Conducting Polypyrrole Films. *Anal. Chim. Acta* **2004**, *502*, 229–234.
- (178) Moraes, M. L.; Rodrigues, U. P.; Oliveira, O. N., Jr.; Ferreira, M. Immobilization of Uricase in Layer-by-Layer Films Used in Amperometric Biosensors for Uric Acid. *J. Solid State Electrochem.* **2007**, *11*, 1489–1495.
- (179) Zanon, N. C. M.; Oliveira, O. N., Jr.; Caseli, L. Immobilization of Uricase Enzyme in Langmuir and Langmuir–Blodgett Films of Fatty Acids: Possible Use as a Uric Acid Sensor. *J. Colloid Interface Sci.* **2012**, *373*, 69–74.
- (180) Lakard, B.; Herlem, G.; Lakard, S.; Antoniou, A.; Fahys, B. Urea Potentiometric Biosensor Based on Modified Electrodes with Urease Immobilized on Polyethylenimine Films. *Biosens. Bioelectron.* **2004**, *19*, 1641–1647.
- (181) Rajesh; Bisht, V.; Takashima, W.; Kaneto, K. An Amperometric Urea Biosensor Based on Covalent Immobilization of Urease onto an Electrochemically Prepared Copolymer Poly(N-3-aminopropyl pyrrole-co-pyrrole) Film. *Biomaterials* **2005**, *26*, 3683–3690.
- (182) Crespilho, F. N.; Iost, R. M.; Travain, S. A.; Oliveira, O. N., Jr.; Zucolotto, V. Enzyme Immobilization on Ag Nanoparticles/Polyaniline Nanocomposites. *Biosens. Bioelectron.* **2009**, *24*, 3073–3077.
- (183) Wang, C. S.; Zheng, J. Y.; Oliveira, O. N., Jr.; Leblanc, R. M. Nature of the Interaction Between a Peptidolipid Langmuir Monolayer and Paraoxon in the Subphase. *J. Phys. Chem. C* **2007**, *111*, 7826–7833.
- (184) Lee, W. C.; Chun, B. S.; Oh, B. K.; Lee, W. H.; Choi, J. W. Fabrication of Protein A-Violagen Hetero Langmuir–Blodgett Film for Fluorescence Immunoassay. *Biotechnol. Bioprocess Eng.* **2004**, *9*, 241–244.
- (185) Garbers, E.; Mitlohner, R.; Georgieva, R.; Baumler, H. Activity of Immobilized Trypsin in the Layer Structure of Polyelectrolyte Microcapsules (PEMC). *Macromol. Biosci.* **2007**, *7*, 1243–1249.
- (186) Ferreira, M.; Fiorito, P. A.; Oliveira, O. N., Jr.; de Torresi, S. I. C. Enzyme-Mediated Amperometric Biosensors Prepared with the Layer-by-Layer (LbL) Adsorption Technique. *Biosens. Bioelectron.* **2004**, *19*, 1611–1615.
- (187) Caseli, L.; dos Santos, D. S.; Foschini, M.; Goncalves, D.; Oliveira, O. N., Jr. The Effect of the Layer Structure on the Activity of Immobilized Enzymes in Ultrathin Films. *J. Colloid Interface Sci.* **2006**, *303*, 326–331.
- (188) Li, Z. S.; Ruan, W. D.; Song, W.; Xue, X. X.; Mao, Z.; Ji, W.; Zhao, B. SERS Detection of Protein Biochip Fabricated by Etching Polystyrene Template. *Spectrochim. Acta, Part A* **2011**, *82*, 456–460.
- (189) Ngoepe, M.; Choonara, Y. E.; Tyagi, C.; Tomar, L. K.; du Toit, L. C.; Kumar, P.; Ndesendo, V. M. K.; Pillay, V. Integration of Biosensors and Drug Delivery Technologies for Early Detection and Chronic Management of Illness. *Sensors* **2013**, *13*, 7680–7713.
- (190) Ryou, M.; Netniroski, A.; Azagury, D.; Shaikh, S. N.; Ryan, M. B.; Westervelt, R. M.; Thompson, C. C. An Implantable Wireless Biosensor for the Immediate Detection of Upper GI Bleeding: A New Fluorescein-Based Tool for Diagnosis and Surveillance. *Gastrointest. Endosc.* **2011**, *74*, 189–194.
- (191) Tan, E. L.; Pereles, B. D.; Horton, B.; Shao, R.; Zourob, M.; Ong, K. G. Implantable Biosensors for Real-Time Strain and Pressure Monitoring. *Sensors* **2008**, *8*, 6396–6406.
- (192) Siontorou, C. G.; Batzias, F. A. Carbohydrate Detection Failure Analysis via Biosensing. *IEEE Trans. Instrum. Meas.* **2008**, *57*, 2856–2867.
- (193) Muren, N. B.; Barton, J. K. Electrochemical Assay for the Signal-On Detection of Human DNA Methyltransferase Activity. *J. Am. Chem. Soc.* **2013**, *135*, 16632–16640.
- (194) Pheeney, C. G.; Arnold, A. R.; Grodick, M. A.; Barton, J. K. Multiplexed Electrochemistry of DNA-Bound Metalloproteins. *J. Am. Chem. Soc.* **2013**, *135*, 11869–11878.
- (195) Komor, A. C.; Barton, J. K. The Path for Metal Complexes to a DNA Target. *Chem. Commun.* **2013**, *49*, 3617–3630.
- (196) Lymberis, A. Progress in R&D on Wearable and Implantable Biomedical Sensors for Better Healthcare and Medicine. *Eng. Med. Biol. Soc.* **2005**, 296–298.
- (197) Heathfield, H. A.; Wyatt, J. Philosophies for the Design and Development of Clinical Decision-Support Systems. *Method Inf. Med.* **1993**, *32*, 1–8.
- (198) Marx, V. Biology: The Big Challenges of Big Data. *Nature* **2013**, *498*, 255–260.
- (199) Maestre, C.; Quilis, J. D. S.; Torres, E.; Blanquer, I.; Medina, R.; Hernandez, V.; Marti, L. Assessing the Usability of a Science Gateway for Medical Knowledge Bases with TRENCADIS. *J. Grid. Comput.* **2012**, *10*, 665–688.
- (200) Xia, J. G.; Lyle, N. H.; Mayer, M. L.; Pena, O. M.; Hancock, R. E. W. INVEX—A Web-based Tool for Integrative Visualization of Expression Data. *Bioinformatics* **2013**, *29*, 3232–3234.
- (201) Statnikov, A.; Aliferis, C. F.; Tsamardinos, I.; Hardin, D.; Levy, S. A Comprehensive Evaluation of Multicategory Classification Methods for Microarray Gene Expression Cancer Diagnosis. *Bioinformatics* **2005**, *21*, 631–643.
- (202) Portet, F.; Reiter, E.; Gatt, A.; Hunter, J.; Sripada, S.; Freer, Y.; Sykes, C. Automatic Generation of Textual Summaries from Neonatal Intensive Care Data. *Artif. Intell.* **2009**, *173*, 789–816.
- (203) Oliveira, O. N., Jr.; Pavinatto, F. J.; Constantino, C. J. L.; Paulovich, F. V.; de Oliveira, M. C. F. Information Visualization to Enhance Sensitivity and Selectivity in Biosensing. *Biointerphases* **2012**, *7*, 1–4.
- (204) Diamond, D. Internet-Scale Sensing. *Anal. Chem.* **2004**, *76*, 278a–286a.
- (205) Diamond, D.; Coyle, S.; Scarmagnani, S.; Hayes, J. Wireless Sensor Networks and Chemo-/Biosensing. *Chem. Rev.* **2008**, *108*, 652–679.
- (206) Bishop, C. M. *Neural Networks for Patterning Recognition*; Clarendon Press: Oxford, 2005.
- (207) Gehlenborg, N.; O'Donoghue, S. I.; Baliga, N. S.; Goesmann, A.; Hibbs, M. A.; Kitano, H.; Kohlbacher, O.; Neuweger, H.; Schneider, R.; Tenenbaum, D.; Gavin, A. C. Visualization of Omics Data for Systems Biology. *Nat. Methods* **2010**, *7*, 56–68.
- (208) Walter, T.; Shattuck, D. W.; Baldock, R.; Bastin, M. E.; Carpenter, A. E.; Duce, S.; Ellenberg, J.; Fraser, A.; Hamilton, N.; Pieper, S.; Ragan, M. A.; Schneider, J. E.; Tomancak, P.; Heriche, J. K. Visualization of Image Data from Cells to Organisms. *Nat. Methods* **2010**, *7*, 26–41.
- (209) Ferreira, E. J.; Pereira, R. C. T.; Delbem, A. C. B.; Oliveira, O. N., Jr.; Mattoso, L. H. C. Random Subspace Method for Analysing Coffee with Electronic Tongue. *Electron. Lett.* **2007**, *43*, 1138–1140.
- (210) Kurnik, R. T.; Oliver, J. J.; Waterhouse, S. R.; Dunn, T.; Jayalakshmi, Y.; Lesho, M.; Lopatin, M.; Tamada, J.; Wei, C.; Potts, R. O. Application of the Mixtures of Experts Algorithm for Signal Processing in a Noninvasive Glucose Monitoring System. *Sens. Actuators, B* **1999**, *60*, 19–26.
- (211) Weiging, Y.; Chen, J.; When, X.; Qingshen, J.; Yang, J.; Su, Y.; Zhu, G.; Wu, W.; Wang, Z. L. Triboelectrification Based Motion Sensor for Human–Machine Interfacing. *ACS Appl. Mater. Interfaces* **2014**, *6*, 7479–7484.
- (212) Gupta, R.; Reifengerger, R. G.; Kulkarni, G. U. Cellphone Camera Imaging of a Periodically Patterned Chip as a Potential Method for Point-of-Care Diagnostics. *ACS Appl. Mater. Interfaces* **2014**, *6*, 3923–3929.

(213) Geladi, P.; Nelson, A.; Lindholm-Sethson, B. Complex Numbers in Chemometrics—Examples from Multivariate Impedance Measurements on Lipid Monolayers. *Anal. Chim. Acta* **2007**, *595*, 152–159.

(214) Lindholm-Sethson, B.; Nystrom, J.; Malmsten, M.; Ringstad, L.; Nelson, A.; Geladi, P. Electrochemical Impedance Spectroscopy in Label-Free Biosensor Applications: Multivariate Data Analysis for an Objective Interpretation. *Anal. Bioanal. Chem.* **2010**, *398*, 2341–2349.

(215) Torgerson, W. S. Multidimensional Scaling of Similarity. *Psychometrika* **1965**, *30*, 379–393.

(216) Jolliffe, I. *Principal Component Analysis*; Springer-Verlag Press: New York, 2002.

(217) Minghim, R.; Paulovich, F. V.; Lopes, A. A. Content-based text mapping using multidimensional projections for exploration of document collections. *IS&T/SPIE Symp. Electron. Imaging* **2006**, *6060*, S1–S12.

(218) Moraes, M. L.; Rodrigues, V. C.; Soares, J. C.; Ferreira, M.; de Souza, N. C.; Oliveira, O. N., Jr. Immunosensor for HIV-1 Diagnostics Based on Immobilization of the Antigenic Peptide P24-3 into Liposomes. *J. Nanosci. Nanotechnol.* **2014**, *14*, 6638–6645.

(219) Moraes, M. L.; Petri, L.; Oliveira, V.; Olivati, C. A.; de Oliveira, M. C. F.; Paulovich, F. V.; Oliveira, O. N., Jr.; Ferreira, M. Detection of Glucose and Triglycerides Using Information Visualization Methods To Process Impedance Spectroscopy Data. *Sens. Actuators, B* **2012**, *166*, 231–238.

(220) Siqueira, J. R., Jr.; Maki, R. M.; Paulovich, F. V.; Werner, C. F.; Poghossian, A.; de Oliveira, M. C. F.; Zucolotto, V.; Oliveira, O. N., Jr.; Schöning, M. J. Use of Information Visualization Methods Eliminating Cross Talk in Multiple Sensing Units Investigated for a Light-Addressable Potentiometric Sensor. *Anal. Chem.* **2010**, *82*, 61–65.

(221) Aoki, P. H. B.; Carreon, E. G. E.; Volpati, D.; Shimabukuro, M. H.; Constantino, C. J. L.; Aroca, R. F.; Oliveira, O. N., Jr.; Paulovich, F. V. SERS Mapping in Langmuir–Blodgett Films and Single-Molecule Detection. *Appl. Spectrosc.* **2013**, *67*, 563–569.